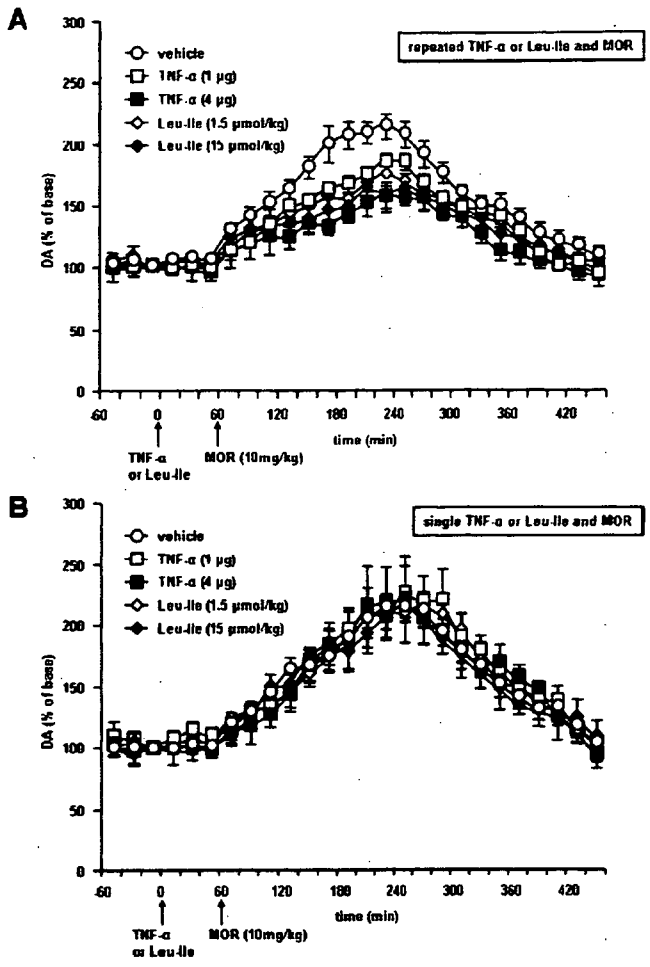

Figure 7. Effects of TNF-α or Leu-Ile on MOR-induced increase in extracellular DA levels. **(A)** Effect of exogenous TNF-α or Leu-Ile on the repeated MOR treatment-induced increase in extracellular DA levels. Mice were treated with TNF-α (1 and 4 μg, IP) or Leu-Ile (1.5 and 15 μmol/kg, IP) 1 hour before MOR (10 mg/kg, SC) once a day for 9 days. Extracellular levels of DA were measured in the NAc by in vivo microdialysis. Basal extracellular DA levels were 3.1 ± .4, 3.0 ± .4, 2.8 ± .3, 2.8 ± .4, and 3.0 ± .5 pg/20 μL for the vehicle/MOR-, TNF-α 1 μg/MOR-, TNF-α 4 μg/MOR-, Leu-Ile 1.5 μmol/MOR-, and Leu-Ile 15 μmol/MOR-treated mice, respectively. Values are means ± SEM (n = 5–7). Analysis of variance with repeated measures revealed significant differences in extracellular DA levels. **(B)** Effect of exogenous TNF-α or Leu-Ile on the single MOR treatment-induced increase in extracellular DA levels. Mice were treated with TNF-α (1 and 4 μg, IP) or Leu-Ile (1.5 and 15 μmol/kg, IP) once 1 hour before MOR (10 mg/kg, SC). Extracellular levels of DA were measured in the NAc by in vivo microdialysis. Basal extracellular DA levels were 2.1 ± .4, 1.9 ± .2, 2.0 ± .2, 1.9 ± .2, and 1.8 ± .2 pg/20 μL for the vehicle/MOR-, TNF-α 1 μg/MOR-, TNF-α 4 μg/MOR-, Leu-Ile 1.5 μmol/MOR-, and Leu-Ile 15 μmol/MOR-treated mice, respectively. Values are means ± SEM (n = 5–6). Analysis of variance with repeated measures revealed no significant differences in extracellular DA levels. TNF-α, tumor necrosis factor-α; MOR, morphine; DA, dopamine; IP, intraperitoneal; SC, subcutaneous; NAc, nucleus accumbens.

best exemplified when studying the antinociceptive or rewarding effects of MOR (Di Chiara and North 1992; Laakso *et al.* 2002).

We examined the influence of TNF-α or Leu-Ile on the antinociceptive effect of MOR in a hot plate test. As shown in Figure 8A, there was no difference in hot plate latency by co-administration of vehicle, TNF-α (1 and 4 μg, IP), or Leu-Ile (1.5 and 15 μmol/kg, IP) with single and repeated MOR (10

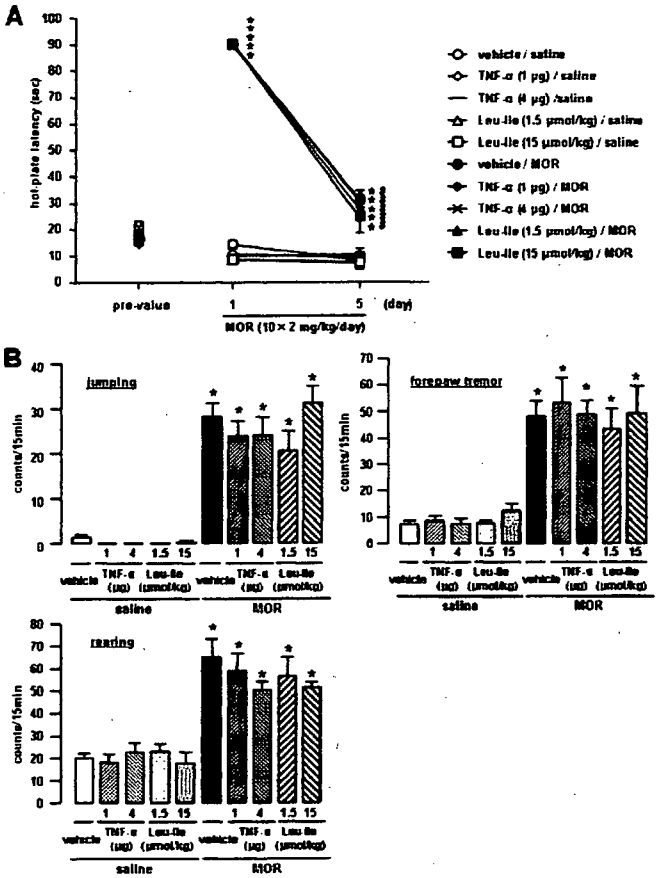

Figure 8. Effects of TNF-α or Leu-Ile on the MOR-induced antinociceptive effects and symptoms of withdrawal. **(A)** Effects of TNF-α or Leu-Ile on the antinociceptive effect and tolerance induced by repeated MOR treatment. Mice were treated with TNF-α (1 and 4 μg, IP) or Leu-Ile (1.5 and 15 μmol/kg, IP) 1 hour before MOR (10 mg/kg, SC) twice a day for 5 days. The analgesic effect of MOR was determined 60 min after the first MOR treatment on day 1 and the second MOR treatment on day 5. Values are means ± SEM (n = 6–10). *p < .05 versus vehicle/saline-treated mice on the first day. *p < .05 versus vehicle/MOR-treated mice on the first day. **(B)** Effects of repeated co-administration of TNF-α or Leu-Ile with MOR on naloxone-precipitated (NAL; 5 mg/kg, IP) withdrawal symptoms. Mice were treated with TNF-α (1 and 4 μg, IP) or Leu-Ile (1.5 and 15 μmol/kg, IP) 1 hour before MOR (10 mg/kg, SC) twice a day for 5 days. On the sixth day, mice were treated with TNF-α (1 and 4 μg, IP) or Leu-Ile (1.5 and 15 μmol/kg, IP) and NAL (5 mg/kg, IP) 1 hour before and 2 hours after MOR (10 mg/kg, SC) treatment, respectively. Immediately after the NAL treatment, NAL-precipitated MOR withdrawal symptoms (jumping, forepaw tremor, rearing) were enumerated manually for 15 min. Saline-precipitated MOR withdrawal symptoms: [jumping] .00 ± .00 (vehicle/saline), .00 ± .00 (TNF-α 1 μg/saline), .00 ± .00 (TNF-α 4 μg/saline), .00 ± .00 (Leu-Ile 1.5 μmol/saline), .00 ± .00 (Leu-Ile 15 μmol/saline), .10 ± .00 (vehicle/MOR), .00 ± .00 (TNF-α 1 μg/MOR), .00 ± .00 (TNF-α 4 μg/MOR), .00 ± .00 (Leu-Ile 1.5 μmol/MOR), .00 ± .00 (Leu-Ile 15 μmol/MOR); [forepaw tremor] 9.00 ± 1.28 (vehicle/saline), 10.00 ± 1.06 (TNF-α μg/saline), 12.83 ± 1.64 (TNF-α 4 μg/saline), 9.70 ± 1.40 (Leu-Ile 1.5 μmol/saline), 13.81 ± 1.80 (Leu-Ile 15 μmol/saline), 14.60 ± 2.24 (vehicle/MOR), 12.67 ± 1.74 (TNF-α 1 μg/MOR), 13.50 ± 2.32 (TNF-α 4 μg/MOR), 13.60 ± 1.97 (Leu-Ile 1.5 μmol/MOR), 12.00 ± 2.63 (Leu-Ile 15 μmol/MOR); [rearing] 34.30 ± 2.38 (vehicle/saline), 29.33 ± 4.47 (TNF-α 1 μg/saline), 30.00 ± 3.57 (TNF-α 4 μg/saline), 28.60 ± 3.25 (Leu-Ile 1.5 μmol/saline), 32.17 ± 1.89 (Leu-Ile 15 μmol/saline), 42.60 ± 5.48 (vehicle/MOR), 38.50 ± 2.72 (TNF-α 1 μg/MOR), 39.17 ± 3.27 (TNF-α 4 μg/MOR), 38.40 ± 3.01 (Leu-Ile 1.5 μmol/MOR), 32.50 ± 2.79 (Leu-Ile 15 μmol/MOR). Values are means ± SEM (n = 6–10). *p < .05 versus vehicle/saline-treated mice. TNF-α, tumor necrosis factor-α; MOR, morphine; IP, intraperitoneal; SC, subcutaneous; NAL, naloxone.

mg/kg, SC). In addition, a tolerance in the analgesic effects of MOR to thermal stimuli was developed in all MOR-treated mice [$F(2,27) = 383.976$, $F(2,15) = 277.874$, $F(2,15) = 723.622$, $F(2,27) = 517.466$, $F(2,15) = 112.064$, $p < .05$, one-way ANOVA] (Figure 8A).

Finally, we investigated the effects of repeated co-administration of TNF-α or Leu-Ile with MOR on NAL-precipitated withdrawal. Withdrawal symptoms (jumping, forepaw tremor, rearing) after treatment with NAL (5mg/kg, IP) were shown in all repeated MOR-treated (10 × 2 mg/kg/day for 5 days) mice [$F(9,66) = 22.846$, $F(9,66) = 13.938$, $F(9,66) = 10.676$, $p < .05$, one-way ANOVA]. There was no difference in the NAL-precipitated withdrawal syndrome by co-administration of vehicle, TNF-α (1 and 4 μg/day for 5 days, IP), or Leu-Ile (1.5 and 15 μmol/kg/day for 5 days, IP) with repeated MOR (10 mg/kg, SC) (Figure 8B).

Discussion

Drugs of abuse are able to elicit compulsive drug-seeking behaviors on repeated administration, which ultimately leads to the phenomenon of addiction (Laakso *et al.* 2002). In terms of lost lives and productivity, drug addiction remains one of the most serious threats to the nation's public health (Nestler 2002).

Recently, we have demonstrated that TNF-α or Leu-Ile, which induces GDNF production via TNF-α synthesis, inhibits METH-induced dependence (Nakajima *et al.* 2004; Niwa *et al*, in press). Morphine is a drug of abuse like METH, although they have opposite effects, acting as a psychosedative and psychostimulant, respectively. In the present study, to extend our findings, we examined the effects of TNF-α or Leu-Ile on the rewarding effect, the sensitization to the locomotor-stimulating effects, and the increase in extracellular DA levels induced by MOR.

Although single MOR treatment did not induce expression of TNF-α mRNA in any regions examined, repeated MOR treatment remarkably induced it in the NAc and CPu (Figure 2A). Moreover, we confirmed TNF-α protein was not increased after single treatment of MOR using immunostaining method (data not shown). We suggest that the induction of TNF-α by MOR requires repeated treatment. The MOR-induced increase in the expression of TNF-α mRNA in the NAc was completely inhibited by pretreatment with the DA D1 receptor antagonist SCH23390, the D2 receptor antagonist raclopride (Figure 2B), and the specific opioid receptor antagonist NAL (Figure 2C), suggesting that the activation of DA D1, D2, and opioid receptors is attributable to MOR-induced gene expression of TNF-α. It is likely that activation of DA transmission in neurons, where TNF-α specifically acts (Figure 3B), is necessary for MOR-induced TNF-α expression. The expression of TNF-α is induced through the activation of transcription factors such as activator protein-1 (AP-1) and nuclear factor-κB (NF-κB) by the activation of JNK/p38 MAPK (Guha *et al.* 2000; Rahman and MacNee 2000). Further, TNF-α acts on mitochondria to generate reactive oxygen species (ROS), which are involved in the activation of AP-1 and NF-κB (Rahman and MacNee 2000). Changes in transcription factors may result in long-term changes in gene expression, thereby contributing to neuronal adaptations that underlie behavioral sensitization (Nestler 2001).

Tumor necrosis factor-α induces GDNF expression (Niwa *et al*, in press) and blocks METH-induced dependence (Nakajima *et al.* 2004). Tumor necrosis factor-α or Leu-Ile treatment, both in combination with MOR and after withdrawal from repeated treatment with MOR, inhibited place preference and sensitization to MOR (Figures 4 and 5). Therefore, we investigated whether Leu-Ile, which is a GDNF inducer, induces the expression of TNF-α. Leu-Ile increased TNF-α mRNA levels in the NAc (Figure 3A). Leu-Ile treatment, both in combination with MOR and after withdrawal from repeated treatment with MOR, also increased TNF-α levels (Figures 3B, 3C, and 3D) in the brain but not in the peripheral blood stream (Niwa *et al*, in press). Leu-Ile can penetrate the blood-brain barrier (BBB) and initiate the synthesis of GDNF in the brain (Nitta *et al.* 2004). Therefore, we suggest that Leu-Ile penetrates the BBB and induces TNF-α expression only in the brain. Therefore, we suggest that Leu-Ile plays an inhibitory role in rewarding effects and sensitization induced by MOR via the induction of TNF-α expression.

Tumor necrosis factor-α-(-/-) mice showed marked conditioned place preference at the low dose of MOR, which failed to establish place preference in wild-type mice (Figure 6A). Morphine-induced place preference in TNF-α-(-/-) mice was significantly attenuated by the administration of TNF-α (Figure 6B). These results suggest that TNF-α acts to negate the rewarding effects of MOR.

From the point of view of pharmacotherapy, Leu-Ile would be better than TNF-α itself, since TNF-α damages the peripheral tissues by triggering the expression of other cytokines (Bluthe *et al.* 1994). Tumor necrosis factor-α could be involved in the inhibitory effects of Leu-Ile on MOR-induced rewarding effects, since no effect of Leu-Ile was observed in the TNF-α-(-/-) mice (Figure 6B). Our results showed that Leu-Ile, which induces GDNF production via TNF-α synthesis, inhibited MOR-induced place preference and sensitization not only during, but also after, their development (Figures 4 and 5), as in the case of METH (Niwa *et al*, in press). Glial cell line-derived neurotrophic factor levels in the NAc after the co-administration of Leu-Ile and MOR were much more increased compared with those in the vehicle/MOR-treated mice (Niwa *et al.* 2006, unpublished observations). Glial cell line-derived neurotrophic factor could be involved in the inhibitory effects of Leu-Ile on MOR-induced rewarding effects, since no effect of Leu-Ile was observed in the GDNF heterozygous mice (Niwa *et al.* 2006, unpublished observations). These results suggest that GDNF acts to negate the rewarding effects of MOR and are involved in the effects of Leu-Ile on rewarding effects. Glial cell line-derived neurotrophic factor blocks biochemical adaptations to the chronic use of cocaine or MOR, as well as the rewarding effects of cocaine (Messer *et al.* 2000). Therefore, Leu-Ile may induce production of GDNF as a result of TNF-α expression to inhibit drug-induced rewarding effects and sensitization, although another pathway should be considered—that Leu-Ile upregulates GDNF expression by activating heat shock protein 90 (Hsp90)/Akt/cyclic adenosine 3', 5'-monophosphase (cAMP) response element binding protein (CREB) signaling (Cen *et al.* 2006).

Leu-Ile inhibited MOR-induced place preference (Figures 5A) in bell-shaped response curves. We confirmed that Leu-Ile at the lower dose, 1.5 μmol/kg, which could inhibit the rewarding effects of MOR, increased TNF-α expression both in combination with MOR and after withdrawal from repeated MOR treatment in the CPP paradigm. On the contrary, Leu-Ile at the higher dose, 15 μmol/kg, which could not inhibit the rewarding effects of MOR, failed to increase TNF-α expression in combination with MOR in the CPP paradigm (data not shown). These results suggest involvement of induction of TNF-α expression in inhibitory effect of Leu-Ile on the rewarding effects and sensitization of MOR.

There has been considerable progress in identifying the mechanisms that contribute to the long-lasting neural and behav-

ioral plasticity related to addiction, including drug-induced changes in gene transcription, in RNA and protein processing, and in synaptic structure (Nestler 2001). Although a single administration of TNF-α or Leu-Ile failed to inhibit the single treatment-induced hyperlocomotion, it inhibited the sensitization to hyperlocomotion induced by repeated treatment with MOR (Figures 4A and 4B). These results suggest that TNF-α or Leu-Ile has inhibitory effects on neuronal plasticity induced by repeated MOR treatment but not on hyperlocomotion or the increase in extracellular DA levels induced by single MOR treatment (Figure 7B). Several reports have suggested that TNF-α influences synaptic strength and transmission (Albensi and Mattson 2000; Beattie *et al.* 2002). Further, the expression of TNF-α is induced through the activation of transcription factors such as AP-1 and NF-κB (Guha *et al.* 2000; Rahman and MacNee 2000). Our results have shown that Leu-Ile binds heat shock cognate protein (Hsc70) and triggers the phosphorylation of NF-κB and CREB via a pathway involving Hsp90/Akt and induces GDNF expression (Cen *et al.* 2006). We suggest that the induction of TNF-α and GDNF by Leu-Ile requires repeated treatment, and these molecules inhibit MOR-induced rewarding effects and sensitization.

The mesolimbic dopamine system projecting from the VTA to NAc is considered to play a major role in mediating the rewarding effects of electrical stimulation of the brain and drugs of abuse (Koob *et al.* 1998). The VTA and NAc have been shown to be the key brain regions that underlie the actions of opioids (e.g., MOR) and psychostimulants (e.g., METH and cocaine) (Koob 1992). It is well recognized that the rewarding effects of opioids and psychomotor stimulants depend on the mesocorticolimbic dopamine system innervating the NAc (Everitt and Wolf 2002; Koob *et al.* 1998; Mizoguchi *et al.* 2004). It has been suggested that the enhancement of DA release in the NAc is an essential process related to the rewarding effects of MOR (Matthews and German 1984). Further, the NAc is involved in the locomotor-stimulating effect of MOR (Brase *et al.* 1977; Oliverio *et al.* 1975), which is regarded as a result of the increase in extracellular DA levels (Koob and Nestler 1997; Matthews and German 1984). We have recently demonstrated that the tissue plasminogen activator (tPA)-plasmin system participates in the rewarding and locomotor-stimulating effects induced not only by MOR but also by METH by triggering the release of dopamine in the NAc (Nagai *et al.* 2004, 2005a, 2005b; Yamada *et al.* 2005). Leu-Ile inhibited the sensitization of hyperlocomotion induced not only by MOR (Figures 4B and 4C) but also by METH (Niwa *et al*, in press), at least in part, through the action in the NAc, since it had inhibitory effects on the repeated MOR treatment-induced increase in extracellular DA levels (Figure 7A). Leu-Ile induces the expression of not only TNF-α (Figure 3A) but also GDNF (Niwa *et al*, in press). Tumor necrosis factor-α induced by Leu-Ile activates plasmalemmal and vesicular DA transporter (Nakajima *et al.* 2004). Glial cell line-derived neurotrophic factor induced by Leu-Ile inhibits the drug-induced upregulation of tyrosine hydroxylase activity (Messer *et al.* 2000). Thereby, TNF-α and GDNF induced by Leu-Ile attenuate the MOR-induced increase in extracellular DA levels (Figure 7A) and then inhibit MOR-induced rewarding effect and sensitization (Figures 4 and 5).

Chronic use of an opioid results in tolerance to and dependence on the drug (Chavkin and Goldstein 1984; Law *et al.* 1982; Puttfarcken *et al.* 1988). Dependence is defined by a number of abnormal responses after the abrupt withdrawal of a drug (Johnson and Flemming 1989). Tumor necrosis factor-α or Leu-Ile has no effect on MOR-induced tolerance and physical dependence (Figure 8). Tumor necrosis factor-α or Leu-Ile regulates dopaminergic neurons, at least in part, through action in the NAc, whereas the cortex is the terminal/intermedial area for noradrenergic neurons associated with drug addiction and plays a key role in NAL-precipitated MOR withdrawal (Terwilliger *et al.* 1991). Therefore, the mechanism by which TNF-α or Leu-Ile inhibits MOR-induced rewarding effect and sensitization is different from that of the NAL-precipitated MOR withdrawal syndrome.

Our findings suggest that TNF-α inhibits MOR-induced rewarding effect and sensitization by attenuating the MOR-induced increase in extracellular DA levels, and Leu-Ile inhibits them via the induction of TNF-α expression. Leu-Ile could be a novel therapeutic agent for MOR-induced dependence.

This study was supported in part by a Grant-in-aid for Scientific Research and Special Coordination Funds for Promoting Science and Technology, Target-Oriented Brain Science Research Program; by a Grant-in-aid for Scientific Research (B) and Young Scientists (A); by the 21st Century Center of Excellence Program "Integrated Molecular Medicine for Neuronal and Neoplastic Disorders" from the Ministry of Education, Culture, Sports, Science and Technology of Japan; by a Grant-in-aid for Health Science Research on Regulatory Science of Pharmaceuticals and Medical Devices, and Comprehensive Research on Aging and Health from the Ministry of Health, Labor and Welfare of Japan; by a Smoking Research Foundation Grant for Biomedical Research; by the Mochida Memorial Foundation for Medical and Pharmaceutical Research; by a grant from the Brain Research Center from 21st Century Frontier Research Program funded by the Ministry of Science and Technology, Republic of Korea; and by Japan Canada Joint Health Research Program.

We are grateful to Dainippon Pharmaceutical Co., Ltd. for the supply of recombinant human TNF-α.

Albensi BC, Mattson MP (2000): Evidence for the involvement of TNF and NF-kappaB in hippocampal synaptic plasticity. *Synapse* 35:151–159.

Aloe L, Fiore M (1997): TNF-α expressed in the brain of transgenic mice lowers central tyrosine hydroxylase immunoreactivity and alters grooming behavior. *Neurosci Lett* 238:65–68.

Beattie EC, Stellwagen D, Morishita W, Bresnahan JC, Ha BK, Von Zastrow M, *et al.* (2002): Control of synaptic strength by glial TNF alpha. *Science* 295:2282–2285.

Bluthe RM, Pawlowski M, Suarez S, Parnet P, Pittman Q, Kelley KW, *et al.* (1994): Synergy between tumor necrosis factor alpha and interleukin-1 in the induction of sickness behavior in mice. *Psychoneuroendocrinology* 19:197–207.

Bonci A, Williams JT (1997): Increased probability of GABA release during withdrawal from morphine. *J Neurosci* 17:796–803.

Boudreau AC, Wolf ME (2005): Behavioral sensitization to cocaine is associated with increased AMPA receptor surface expression in the nucleus accumbens. *J Neurosci* 25:9144–9151.

Brase DA, Loh HH, Way EL (1977): Comparison of the effects of morphine on locomotor activity, analgesia and primary and protracted physical dependence in six mouse strains. *J Pharmacol Exp Ther* 201:368–374.

Cen X, Nitta A, Ohya S, Zhao Y, Ozawa N, Mouri A, *et al.* (2006): An analogue of dipeptide-like structure of FK506 increases GDNF expression through CREB activated by Hsp90/Akt signaling pathway. *J Neurosci* 26:3335–3344.

Chavkin C, Goldstein A (1984): Opioid receptor reserve in normal and morphine-tolerant guinea pig ileum myenteric plexus. *Proc Natl Acad Sci U S A* 81:7253–7257.

Di Chiara G, North RA (1992): Neurobiology of opioid abuse. *Trends Pharmacol Sci* 13:185–193.

Everitt BJ, Wolf ME (2002): Psychomotor stimulant addiction: A neural systems perspective. *J Neurosci* 22:3312–3320.

Franklin KBJ, Paxinos G (1997): *The Mouse Brain in Stereotaxic Coordinates.* San Diego: Academic press.

Funada M, Suzuki T, Narita M, Misawa M, Nagase H (1993): Blockade of morphine reward through the activation of κ-opioid receptors in mice. *Neuropharmacology* 32:1315–1323.

Giros B, Jaber M, Jones SR, Wightman RM, Caron MG (1996): Hyperlocomotion and indifference to cocaine and amphetamine in mice lacking the dopamine transporter. *Nature* 379:606–612.

Guha M, Bai W, Nadler JL, Natarajan R (2000): Molecular mechanisms of tumor necrosis factor alpha gene expression in monocytic cells via hyperglycemia-induced oxidant stress-dependent and -independent pathways. *J Biol Chem* 275:17728–17739.

Hamdy MM, Noda Y, Miyazaki M, Mamiya T, Nozaki A, Nitta A, *et al.* (2004): Molecular mechanisms in dizocilpine-induced attenuation of development of morphine dependence: An association with cortical Ca^{2+}/calmodulin-dependent signal cascade. *Behav Brain Res* 152:263–270.

Heikkila RE, Orlansky H, Cohen G (1975): Studies on the distinction between uptake inhibition and release of ^{3}H-dopamine in rat brain tissue slices. *Biochem Pharmacol* 24:847–852.

Itoh A, Shiotani T, Nakayama S, Mamiya T, Hasegawa T, Noda Y, *et al.* (2000): Attenuation of the development of morphine dependence/tolerance by nefiracetam: Involvement of adenosine 3':5'-cyclic monophosphate system. *Behav Brain Res* 115:65–74.

Johnson SM, Fleming WW (1989): Mechanisms of cellular adaptive sensitivity changes: Applications to opioid tolerance and dependence. *Pharmacol Rev* 41:435–488.

Johnson SW, North RA (1992): Opioids excite dopamine neurons by hyperpolarization of local interneurons. *J Neurosci* 12:483–488.

Kalivas PW, Stewart J (1991): Dopamine transmission in the initiation and expression of drug- and stress-induced sensitization of motor activity. *Brain Res Brain Res Rev* 16:223–244.

Koob GF (1992): Drugs of abuse: Anatomy, pharmacology and function of reward pathways. *Trends Pharmacol Sci* 13:177–184.

Koob GF, Nestler EJ (1997): The neurobiology of drug addiction. *J Neuropsychiatry Clin Neurosci* 9:482–497.

Koob GF, Sanna PP, Bloom FE (1998): Neuroscience of addiction. *Neuron* 21:467–476.

Kuwahara M, Sugimoto M, Tsuji S, Miyata S, Yoshida A (1999): Cytosolic calcium changes in a process of platelet adhesion and cohesion on a von Willebrand factor-coated surface under flow conditions. *Blood* 94:1149–1155.

Laakso A, Mohn AR, Gainetdinov RR, Caron MG (2002): Experimental genetic approaches to addiction. *Neuron* 36:213–228.

Law PY, Hom DS, Loh HH (1982): Loss of opiate receptor activity in neuroblastoma X glioma NG108-15 hybrid cells after chronic opiate treatment. A multiple-step process. *Mol Pharmacol* 22:1–4.

Maier SF, Watkins LR (1998): Cytokines for psychologists: Implications of bidirectional immune-to-brain communication for understanding behavior, mood, and cognition. *Psychol Rev* 105:83–107.

Mamiya T, Noda Y, Ren X, Hamdy M, Furukawa S, Kameyama T, *et al.* (2001): Involvement of cyclic AMP systems in morphine physical dependence in mice: Prevention of development of morphine dependence by rolipram, a phosphodiesterase 4 inhibitor. *Br J Pharmacol* 132:1111–1117.

Matthews RT, German DC (1984): Electrophysiological evidence for excitation of rat ventral tegmental area dopamine neurons by morphine. *Neuroscience* 11:617–625.

Messer CJ, Eisch AJ, Carlezon WA Jr, Whisler K, Shen L, Wolf DH, *et al.* (2000): Role for GDNF in biochemical and behavioral adaptations to drugs of abuse. *Neuron* 26:247–257.

Miyamoto Y, Yamada K, Nagai T, Mori H, Mishina M, Furukawa H, *et al.* (2004): Behavioral adaptations to addictive drugs in mice lacking the NMDA receptor ε1 subunit. *Eur J Neurosci* 19:151–158.

Mizoguchi H, Yamada K, Mizuno M, Mizuno T, Nitta A, Noda Y, *et al.* (2004): Regulations of methamphetamine reward by extracellular signal-regulated kinase 1/2/ets-like gene-1 signaling pathway via the activation of dopamine receptors. *Mol Pharmacol* 65:1293–1301.

Nagai T, Kamei H, Ito M, Hashimoto K, Takuma K, Nabeshima T, *et al.* (2005a): Modification by the tissue plasminogen activator-plasmin system of morphine-induced dopamine release and hyperlocomotion, but not anti-nociceptive effect in mice. *J Neurochem* 93:1272–1279.

Nagai T, Noda Y, Ishikawa K, Miyamoto Y, Yoshimura M, Ito M, *et al.* (2005b): The role of tissue plasminogen activator in methamphetamine-related reward and sensitization. *J Neurochem* 92:660–667.

Nagai T, Yamada K, Yoshimura M, Ishikawa K, Miyamoto Y, Hashimoto K, *et al.* (2004): The tissue plasminogen activator-plasmin system participates in the rewarding effect of morphine by regulating dopamine release. *Proc Natl Acad Sci U S A* 101:3650–3655.

Nakajima A, Yamada K, Nagai T, Uchiyama T, Miyamoto Y, Mamiya T, *et al.* (2004): Role of tumor necrosis factor-alpha in methamphetamine-induced drug dependence and neurotoxicity. *J Neurosci* 24:2212–2225.

Narita M, Funada M, Suzuki T (2001): Regulations of opioid dependence by opioid receptor types. *Pharmacol Ther* 89:1–15.

Nestler EJ (2001): Molecular basis of long-term plasticity underlying addiction. *Nat Rev Neurosci* 2:119–128.

Nestler EJ (2002): From neurobiology to treatment: Progress against addiction. *Nat Neurosci* 5:1076–1079.

Nitta A, Nishioka H, Fukumitsu H, Furukawa Y, Sugiura H, Shen L, *et al.* (2004): Hydrophobic dipeptide Leu-Ile protects against neuronal death by inducing brain-derived neurotrophic factor and glial cell line-derived neurotrophic factor synthesis. *J Neurosci Res* 78:250–258.

Niwa M, Nitta A, Yamada Y, Nakajima A, Saito K, Seishima M, *et al.*(in press): An inducer for glial cell line-derived neurotrophic factor and tumor necrosis factor-α protects methamphetamine-induced reward and sensitization. *Biol Psychiatry.*

Noda Y, Miyamoto Y, Mamiya T, Kamei H, Furukawa H, Nabeshima T (1998): Involvement of dopaminergic system in phencyclidine-induced place preference in mice pretreated with phencyclidine repeatedly. *J Pharmacol Exp Ther* 286:44–51.

Oliverio A, Castellano C, Eleftheriou BE (1975): Morphine sensitivity and tolerance: A genetic investigation in the mouse. *Psychopharmacologia* 42:219–224.

Puttfarcken PS, Werling LL, Cox BM (1988): Effects of chronic morphine exposure on opioid inhibition of adenylyl cyclase in 7315c cell membranes: A useful model for the study of tolerance at μ opioid receptors. *Mol Pharmacol* 33:520–527.

Rahman I, MacNee W (2000): Regulation of redox glutathione levels and gene transcription in lung inflammation: Therapeutic approaches. *Free Radic Biol Med* 28:1405–1420.

Ren X, Noda Y, Mamiya T, Nagai T, Nabeshima T (2004): A neuroactive steroid, dehydroepiandrosterone sulfate, prevents the development of morphine dependence and tolerance via c-fos expression linked to the extracellular signal-regulated protein kinase. *Behav Brain Res* 152:243–250.

Robinson TE, Berridge KC (2000): The psychology and neurobiology of addiction: An incentive-sensitization view. *Addiction* 95(suppl 2):S91–S117.

Seiden LS, Sabol KE, Ricaurte GA (1993): Amphetamine: Effects on catecholamine systems and behavior. *Annu Rev Pharmacol Toxicol* 33:639–677.

Taniguchi T, Tanaka M, Ikeda A, Momotani E, Sekikawa K (1997): Failure of germinal center formation and impairment of response to endotoxin in tumor necrosis factor α deficient mice. *Lab Invest* 77:647–658.

Terwilliger RZ, Beitner-Johnson D, Sevarino KA, Crain SM, Nestler EJ (1991): A general role for adaptations in G-proteins and the cyclic AMP system in mediating the chronic actions of morphine and cocaine on neuronal function. *Brain Res* 548:100–110.

Tsuji S, Sugimoto M, Miyata S, Kuwahara M, Kinoshita S, Yoshioka A (1999): Real-time analysis of mural thrombus formation in various platelet aggregation disorders: Distinct shear-dependent roles of platelet receptors and adhesive proteins under flow. *Blood* 94:968–975.

Vassali P (1992): The pathophysiology of tumor necrosis factors. *Annu Rev Immunol* 10:411–452.

Vezina P, Stewart J (1984): Conditioning and place-specific sensitization of increases in activity induced by morphine in VTA. *Phamacol Biochem Behav* 20:925–934.

Wada R, Tifft CJ, Proia RL (2000): Microglial activation precedes acute neurodegeneration in Sandhoff disease and is suppressed by bone marrow transplantation. *Proc Natl Acad Sci U S A* 97:10954–10959.

Wise RA (1996): Neurobiology of addiction. *Curr Opin Neurobiol* 6:243–251.

Yamada K, Iida R, Miyamoto Y, Saito K, Sekikawa K, Sedishima M, *et al.* (2000): Neurobehavioral alternations in mice with a targeted deletion of the tumor necrosis factor-alpha gene: Implication for emotional behavior. *J Neuroimmunol* 111:131–138.

Yamada K, Nagai T, Nabeshima T (2005): Drug dependence, synaptic plasticity, and tissue plasminogen activator. *J Pharmacol Sci* 97:157–161.

Behavioral/Systems/Cognitive

A Novel Molecule "Shati" Is Involved in Methamphetamine-Induced Hyperlocomotion, Sensitization, and Conditioned Place Preference

Minae Niwa,[1,3] Atsumi Nitta,[1] Hiroyuki Mizoguchi,[1] Yasutomo Ito,[2] Yukihiro Noda,[1] Taku Nagai,[1] and Toshitaka Nabeshima[1,3]

[1]Department of Neuropsychopharmacology and Hospital Pharmacy and [2]Equipment Center for Research and Education, Nagoya University Graduate School of Medicine, Nagoya 466-8560, Japan, and [3]Department of Chemical Pharmacology, Meijo University Graduate School of Pharmaceutical Sciences, Nagoya 468-8503, Japan

Drug addiction places an enormous burden on society through its repercussions on crime rate and healthcare. Repeated exposure to drugs of abuse causes cellular adaptations in specific neuronal populations that ultimately can lead to a state of addiction. In the present study, we have identified a novel molecule "shati" from the nucleus accumbens (NAc) of mice treated with methamphetamine (METH) using the PCR-select complementary DNA subtraction method. Moreover, we investigated whether shati is involved in METH-induced hyperlocomotion, sensitization, and conditioned place preference (CPP). METH induced expression of shati mRNA dose dependently via dopamine (DA) receptors. We prepared antibodies against shati and, using them, found shati to be expressed in neuronal cells of the mouse brain. Treatment with the shati antisense oligonucleotide (shati-AS), which significantly inhibited the expression of shati mRNA, enhanced the acute METH response, METH-induced behavioral sensitization, and CPP. Blockage of shati mRNA by shati-AS potentiated the METH-induced increase of DA overflow in the NAc and the METH-induced decrease in synaptosomal and vesicular DA uptake in the midbrain. These results suggest that a novel molecule shati is involved in the development of METH-induced hyperlocomotion, sensitization, and CPP. The functional roles of shati in METH-regulated behavioral alternations are likely to be mediated by its inhibitory effects on the METH-induced increase of DA overflow in the NAc and the METH-induced decrease in DA uptake in the midbrain.

Key words: **shati; methamphetamine; behavioral sensitization; conditioned place preference; dopamine; addiction**

Introduction

In terms of lost lives and productivity, drug dependence remains one of the most serious threats to the public health of a nation (Nestler, 2002). Drugs of abuse, including methamphetamine (METH), modulate the activity of mesolimbic dopaminergic neurons, projecting from the ventral tegmental area (VTA) to the nucleus accumbens (NAc) (Koob, 1992; Wise, 1996b; Koob et al., 1998). The psychostimulatory effects of METH are associated with an increase in extracellular dopamine (DA) levels in the brain, by facilitating the release of DA from presynaptic nerve terminals and inhibiting reuptake (Heikkila et al., 1975; Seiden et al., 1993; Giros et al., 1996). In rodent, augmentation of behavioral responses to psychostimulants is observed during and after their repeated administration. Therefore, it has been proposed that activity-dependent synaptic plasticity and remodeling of the mesolimbic dopaminergic system may play a crucial role in drug dependence (Nestler, 2001; Yamada and Nabeshima, 2004).

Using cDNA microarrays, changes in the mRNA expression profile in relevant brain regions (e.g., NAc) have been assessed after chronic administration of abused drugs (Douglass and Daoud, 1996; Cha et al., 1997; Wang et al., 1997). Evidence from this line of research has implicated nuclear factor-κB (Ang et al., 2001) and ΔFosB (Zachariou et al., 2006) in signal transduction pathways that modulate behavioral effects induced by drugs and contribute to long-term neuronal changes associated with dependence (Laakso et al., 2002). To elucidate the mechanism, caused by chronic drug abuse, of stable changes in the brain that play a role in the long-lasting behavioral abnormalities of dependent subjects, the candidates for drug-dependence-related genes

Received Dec. 18, 2006; revised May 21, 2007; accepted May 21, 2007.

This work was supported in part by a Grant-in-Aid for Scientific Research and Special Coordination Funds for Promoting Science and Technology, Target-Oriented Brain Science Research Program; a Grant-in-Aid for Scientific Research (B), Exploratory Research, and Young Scientists (A); the 21st Century Center of Excellence Program "Integrated Molecular Medicine for Neuronal and Neoplastic Disorders" from the Ministry of Education, Culture, Sports, Science, and Technology of Japan; a Grant-in-Aid for Health Science Research on Regulatory Science of Pharmaceuticals and Medical Devices, and Comprehensive Research on Aging and Health from the Ministry of Health, Labor, and Welfare of Japan; a Smoking Research Foundation Grant for Biomedical Research; a grant from the Brain Research Center from the 21st Century Frontier Research Program funded by the Ministry of Science and Technology, Republic of Korea; by the Japan Canada Joint Health Research Program; and by a grant from Takeda Science Foundation. We are grateful to Drs. Kenji Kadomatsu, Yoshifumi Takei, and Hanayo Kawai (Department of Biochemistry, Nagoya University Graduate School of Medicine, Nagoya, Japan) for technical assistance, critical comments, and helpful discussions. We also thank Dr. Noboru Ogiso, Yasutaka Ohya, Yuuki Ushiro, and Kazumi Kawai (Division for Research of Laboratory Animals, Center for Research of Laboratory Animals and Medical Research Engineering, Nagoya University Graduate School of Medicine) and Nobuyoshi Hamada and Yoshiyuki Nakamura (Radioisotope Center Medical Branch, Nagoya University Graduate School of Medicine) for technical assistance.

Correspondence should be addressed to Dr. Toshitaka Nabeshima, Department of Chemical Pharmacology, Meijo University Graduate School of Pharmaceutical Sciences, 150 Yagotoyama, Tenpaku-ku, Nagoya 468-8503, Japan. E-mail: tnabeshi@ccmfs.meijo-u.ac.jp.

DOI:10.1523/JNEUROSCI.1575-07.2007

Copyright © 2007 Society for Neuroscience 0270-6474/07/277604-12$15.00/0

whose expression was altered by repeated administration of METH or morphine (MOR) were screened by using cDNA microarray. Recently, there are many studies that showed that cytokines/neurotrophic factors and extracellular matrix/proteases play critical roles in activity-dependent synaptic plasticity and remodeling of the mesocorticolimbic dopaminergic system (Horger et al., 1999; Messer et al., 2000; Mizoguchi et al., 2007). We found that tumor necrosis factor-α (TNF-α) plays a neuroprotective role in METH-induced dependence and neurotoxicity (Nakajima et al., 2004) and reduces MOR-induced rewarding effects and behavioral sensitization (Niwa et al., 2007a,d). Furthermore, the rewarding effects and sensitization induced by METH and MOR are attenuated by Leu-Ile, an inducer of TNF-α, and glial cell line-derived neurotrophic factor (GDNF) (Niwa et al., 2007a–d). The tissue plasminogen activator (tPA)–plasmin system potentiates the rewarding and locomotor-stimulating effects of METH, MOR, and nicotine by regulating release of DA (Nagai et al., 2004, 2005a,b, 2006). However, the exact neuronal circuits and molecular cascade essential for drug dependence remain unclear. Therefore, we attempt to explore the novel molecules that play more critical roles in drug dependence, because the functions of molecules targeted by DNA microarray screening have been already well known.

In the present study, we identified a novel molecule "shati" from the NAc of mice treated with METH using the PCR-select cDNA subtraction method, which is a differential and epochal cloning technique. Moreover, we demonstrated that shati is involved in the METH-induced hyperlocomotion, sensitization, and conditioned place preference (CPP).

Materials and Methods

Animals. The male C57BL/6J inbred mice were obtained from SLC Japan (Hamamatsu, Japan). Animals were housed in plastic cages and kept in a temperature-, humidity-, and light-controlled room (23 ± 1°C; 50 ± 5% humidity; 12 h light/dark cycle starting at 8:00 A.M.) and had *ad libitum* access to food and water, except during behavioral experiments. All animal care and use was in accordance with the National Institutes of Health *Guide for the Care and Use of Laboratory Animals* and approved by the Institutional Animal Care and Use Committee of Nagoya University School of Medicine. Animals were treated according to the *Guidelines of Experimental Animal Care* issued from the Office of the Prime Minister of Japan.

PCR-select cDNA subtraction. Mice were administered METH (2 mg/kg, s.c.) or saline for 6 d and took NAc 2 h after the last injection of METH. PCR-select cDNA subtraction (Clontech, Palo Alto, CA) was performed using a previously established procedure (Diatchenko et al., 1996; Gurskaya et al., 1996) to detect the genes in the NAc affected by METH treatment. Briefly, they involve hybridization of cDNA from one population (tester; METH-treated NAc) to excess of mRNA (cDNA) from other population (driver; saline-treated NAc) and then separation of the unhybridized fraction (target) from hybridized common sequences. Total RNAs were extracted by RNeasy Max (Qiagen, Hilden, Germany). For each subtraction, we performed two PCR amplifications. Products from the secondary PCRs were inserted into pCRII using a T/A cloning kit (Invitrogen, Carlsbad, CA). Plasmid or cosmid DNAs were prepared using QIAwell 8 Plus kit (Qiagen) according to the protocol of the manufacturer. Nucleic acid homology searches were performed using the BLAST (basic local alignment search tool) program through e-mail servers at the National Center for Biotechnology Information (NCBI) (National Institutes of Health, Bethesda, MD).

Structure models. Homology modeling for C-terminal domain of shati was established using Molecular Operating Environment (MOE) software (Chemical Computing Group, Montreal, Quebec, Canada). Molecular mechanics calculations were performed by using an MMFF94x force field. Docking simulations of acetyl-CoA or ATP with shati protein were also examined using MOE software (Chemical Computing Group) to calculate the interactive potential energy of molecules.

Table 1. Primers sequences and their targets for RT-PCR

Primer	Sequence	Target (bp)
1		
Forward	5′-CTTGCCTCCCCAGCCCATCA-3′	1987–2006
Reverse	5′-CTGGGGGCCAGGGTTCTGCT-3′	2147–2166
2		
Forward	5′-GGGTGGCCGGGTAGGTGGAA-3′	2909–2928
Reverse	5′-GGCAGTGCCCAGCCCTTCCT-3′	3073–3092
3		
Forward	5′-TGTACATTCCTCCCTGGTGGTG-3′	3521–3542
Reverse	5′-AAATCTGAGAGCTGCAAGAAAATAGGG-3′	3594–3620

The amplification consisted of an initial step (95°C for 5 min) and then 35 cycles of denaturation for 30 s at 94 °C and annealing for 1 min at 70, 71, and 65°C.

Reverse transcription-PCR and real-time reverse transcription-PCR. Mice were administered METH (0.3, 1, and 2 mg/kg, s.c., once a day for 3 or 6 d) and decapitated 2 h after the last injection of METH. In the real-time reverse transcription (RT)-PCR experiment on the antagonism of METH-induced shati mRNA expression, mice were treated with the DA D_1-like receptor antagonist *R*(+)-SCH23390 [*R*(+)-7-chloro-8-hydroxy-3-methyl-1-phenyl-2,3,4,5-tetrahydro-1*H*-3-benzazepine] (0.1 mg/kg, i.p.) or DA D_2-like receptor antagonist raclopride (2 mg/kg, i.p.) 30 min before METH (2 mg/kg, s.c.) once a day for 6 d. Functionally, *R*(+)-SCH23390 (0.1–0.5 mg/kg) is a potent blocker of stereotyped behaviors and increased locomotion induced by amphetamine or apomorphine (Christensen et al., 1984; Napier et al., 1986). The increase in TNF-α or tPA mRNA expression in the NAc induced by METH is inhibited by pretreatment with either *R*(+)-SCH23390 (0.1 or 0.5 mg/kg, i.p.) or raclopride (2 mg/kg, i.p.) (Nakajima et al., 2004; Nagai et al., 2005a). *R*(+)-SCH23390 at the dose of 0.1 mg/kg, not 0.03 mg/kg, significantly inhibits the hyperphosphorylation of extracellular signal-regulated kinase 1/2 in the NAc and striatum evoked by METH-induced CPP as well as the expression of CPP in METH-treated animals (Mizoguchi et al., 2004). Depending on these evidences, we selected the doses of *R*(+)-SCH23390 at 0.1 mg/kg and raclopride at 2 mg/kg.

Total RNA was isolated using an RNeasy kit (Qiagen) and converted into cDNA using a SuperScript First-Strand System for RT-PCR kit (Invitrogen). The primers used for RT-PCR were as follows: 5′-CTTGCCTCCCCAGCCCATCA-3′ (forward-1; base pairs 1987–2006) and 5′-CTGGGGGCCAGGGTTCTGCT-3′ (reverse-1; base pairs 2147–2166) for set of sequences 1; 5′-GGGTGGCCGGGTAGGTGGAA-3′ (forward-2; base pairs 2909–2928) and 5′-GGCAGTGCCCAGCCCTTCCT-3′ (reverse-2; base pairs 3073–3092) for set of sequences 2; and 5′-TGTACATTCCTCCCTGGTGGTG-3′ (forward-3; base pairs 3521–3542) and 5′-AAATCTGAGAGCTGCAAGAAAATAGGG-3′ (reverse-3; base pairs 3594–3620) for set of sequences 3 (Table 1). The amplification consisted of an initial step (95°C for 5 min) and then 35 cycles of denaturation for 30 s at 94°C and annealing for 1 min at 70, 71, and 65°C in a GeneAmp PCR System 9700 (Applied Biosystems, Foster City, CA). The levels of shati and TNF-α mRNA were determined by real-time RT-PCR using a TaqMan probe. The 18S ribosomal RNA was used as the internal control (PE Applied Biosystems, Foster City, CA). The mouse shati primers used for real-time RT-PCR were as follows: 5′-TGTAAACACCCCTAAAGTGCCCT-3′ (forward; base pairs 2967–2989) and 5′-TCAATCCTGCATACAAGGAATCAA-3′ (reverse; bare pairs 3022–3045); and TaqMan probe, 5′-CACAGTCTGTGAGGCTCAGGTTGCCC-3′ (probe; base pairs 2995–3020). The amplification consisted of an initial step (95°C for 5 min) and then 40 cycles of denaturation for 30 s at 95°C and annealing for 1 min at 59°C in an iCycle iQ Detection System (Bio-Rad, Hercules, CA). The expression levels were calculated as described previously (Wada et al., 2000).

Immunohistochemistry. Two antibodies against the peptide of the hypothetical protein, CNTAFRGLRQHPRTQLL (S-3) and CMSVDSRFRGKGIAKALG (S-4), unique to shati were generated. These peptides were conjugated to the keyhole limpet hemocyanin and injected into rabbits six times at 1 week intervals. Serum was taken from the rabbits 1

week after the final injection of these peptides. The serum was diluted 200 times used for the immunostaining.

For immunohistochemical analysis, mice were killed 24 h after repeated treatment with METH (2 mg/kg, s.c., once a day for 6 d). The brains were sliced at 20 μm in the cryostat. Polyclonal rabbit anti-S-3 or S-4 antibody (1:200), monoclonal mouse anti-neuron-specific nuclear antigen (NeuN) antibody (1:200; Chemicon, Temecula, CA), and monoclonal mouse anti-glial fibrillary acidic protein (GFAP) antibody (1:200; Chemicon) served as primary antibodies. Goat anti-mouse Alexa Fluor 546 (1:1000; Invitrogen) and goat anti-rabbit Alexa Fluor 488 (1:1000; Invitrogen) were used as secondary antibodies. Each stained slice was observed under a fluorescence microscope (Axioskoop 2 plus; Zeiss, Jena, Germany) and checked with Axiovision 3.0 systems (Zeiss).

Shati-antisense oligonucleotide treatment. Mice were anesthetized with pentobarbital (40 mg/kg, i.p.) and placed in a stereotaxic apparatus. The infusion cannula was connected to a miniosmotic pump (total capacity was 90 μl, Alzet 1002; Alza, Palo Alto, CA) filled with shati-antisense oligonucleotide (shati-AS) and -scramble oligonucleotide (shati-SC) and was implanted into the right ventricle [anteroposterior (AP) −0.5 mm, mediolateral (ML) +1.0 mm from the bregma, and dorsoventral (DV) −2.0 mm from the skull, according to the atlas of Franklin and Paxinos (1997)]. No histological or mechanical disruption was produced by implantation of the infusion cannula (data not shown). Phosphorothionate oligonucleotides were custom synthesized at Nisshinbo Biotechnology (Tokyo, Japan) and dissolved in artificial CSF (in mM: 147 NaCl, 3 KCl, 1.2 $CaCl_2$, and1.0 $MgCl_2$, pH 7.2). We used shati-SC as a control of shati-AS, because we should deny the secondary effects on other genes or toxic effects, and we selected the design of shati-AS, which does not affect the other genes and already have been identified. The oligonucleotides were phosphorothionated at the three bases of both 5′ and 3′ ends, which results in increased stability and less toxicity. The sequences of shati-AS and shati-SC were 5′-TCTTCGTCTCGCAGACCATGTCG-3′ and 5′-GGTCTGCTACACTGCTGCTAGTC-3′, respectively. Shati-AS and shati-SC were continuously infused into the cerebral ventricle at a dose of 1.8 nmol/6 μl per day (flow rate, 0.25 μl/h). Additionally, shati-SC was used as a control. Three days after the start of oligonucleotide infusion, mice were subjected to METH treatment for sensitization.

Locomotor activity. Locomotor activity was measured using an infrared detector (Neuroscience Company, Tokyo, Japan) in a plastic box (32 × 22 × 15 cm high) and determined as described previously (Nakajima et al., 2004; Niwa et al., 2007b,d). One day after the start of oligonucleotide infusion, mice were habituated for 3 h in the box for 2 d and then administered METH (1 mg/kg, s.c.) or saline once a day for 5 d. Locomotor activity was measured for 2 h immediately after the METH or saline administration.

In vivo *microdialysis.* Mice were anesthetized with sodium pentobarbital, and a guide cannula (AG-8; EICOM, Kyoto, Japan) was implanted into the NAc (AP +1.7 mm, ML +0.8 mm mediolateral from the bregma, and DV −4.0 mm from the skull) according to the atlas of Franklin and Paxinos (1997) and secured to the skull using stainless steel screws and dental acrylic cement. Mice were administered METH (1 mg/kg, s.c.) 3 d after implantation of the guide cannula and the start of oligonucleotide infusion. One day after METH treatment for 2 d, a dialysis probe (AI-8-1, 1 mm membrane length; EICOM) was inserted through the guide cannula and perfused continuously with CSF (in mM: 147 NaCl, 4 KCl, and 2.3 $CaCl_2$) at a flow rate of 1.0 μl/min. Dialysate was collected in 20 min fractions and injected into the HPLC system (EICOM) for the measurement of DA levels. Three samples were used to establish baseline levels of DA before the administration of METH (1 mg/kg, s.c.).

Synaptosomal [^{3}H]DA uptake. Three days after the start of oligonucleotide infusion, mice were subjected to METH treatment once a day for 3 d. Mice were decapitated 1 h after the final METH treatment. Midbrain synaptosomal [^{3}H]DA uptake was determined as described previously (Fleckenstein et al., 1997; Nakajima et al., 2004; Niwa et al., 2007b). The final concentration of [^{3}H]DA (PerkinElmer, Wellesley, MA) was 5 nM. Samples were incubated at 37°C for 4 min, and then ice-cold Krebs–Ringer's solution containing 10 μM GBR12909 [1-(2[bis(4-fluorophenyl-)methoxy]ethyl)-4-(3-phenylpropyl)piperazine] bimesylate hydrate] (Sigma, St. Louis, MO), a specific DA uptake inhibitor, was added. Nonspecific values were determined in the presence of 100 μM GBR12909 during the incubation. The radioactivity trapped on filters was measured with a liquid scintillation counter (Beckman Coulter, Fullerton, CA).

Vesicular [^{3}H]DA uptake. Vesicular [^{3}H]DA uptake was determined as described by Erickson et al. (1990). Synaptosomes were prepared as described by Nakajima et al. (2004). Vesicular [^{3}H]DA uptake was performed by incubating synaptic vesicle samples (15 μg protein/100 μl) at 30°C for 4 min in assay buffer (in mM: 25 HEPES, 100 potassium tartrate, 1.7 ascorbic acid, 0.05 EGTA, 0.1 EDTA, and 2 ATP-Mg^{2+}, pH7.0) in the presence of 30 nM [^{3}H]DA (PerkinElmer). The reaction was terminated by the addition of 1 ml of cold wash buffer (assay buffer containing 2 mM $MgSO_4$ substituted for the ATP-Mg^{2+}, pH 7.0) and rapid filtration. Nonspecific values were determined by measuring vesicular [^{3}H]DA uptake at 4°C. The radioactivity was measured with a liquid scintillation counter (Beckman Coulter).

Conditioned place preference. The apparatus used for the place conditioning task consisted of two compartments: a transparent Plexiglas box and a black Plexiglas box (both 15 × 15 × 15 cm high). To enable mice to distinguish easily the two compartments, the floors of the transparent and black boxes were covered with white plastic mesh and black frosting Plexiglas, respectively. Each box could be divided by a sliding door (10 × 15 cm high). The place conditioning paradigm was performed by using a previously established procedure with a minor modification (Noda et al., 1998; Schechter and Calcagnetti, 1998; Niwa et al., 2007a,b,d). In the preconditioning test, the sliding door was opened, and the mouse was allowed to move freely between both boxes for 15 min once a day for 3 d. On the third day of the preconditioning test, we measured the time that the mouse spent in the black and transparent boxes by using a Scanet SV-20 LD (Melquest, Toyama, Japan). The box in which the mouse spent the most time was referred to as the "preferred side" and the other box as the "nonpreferred side." Conditioning was performed during 6 successive days. Mice were given METH or saline in the apparatus with the sliding door closed. That is, a mouse was subcutaneously given METH and put in its nonpreferred side for 20 min. On the next day, the mouse was given saline and placed opposite the drug conditioning site for 20 min. These treatments were repeated for three cycles (6 d). In the postconditioning test, the sliding door was opened, and we measured the time that the mouse spent in the black and transparent boxes for 15 min, using the Scanet SV-20 LD. Place conditioning behavior was expressed by Post-Pre, which was calculated as: [(postvalue) − (prevalue)], where postvalue and prevalue were the difference in time spent at the drug conditioning and the saline conditioning sites in the postconditioning and preconditioning tests, respectively.

Statistical analysis. All data were expressed as means ± SE. Statistical differences between two groups were determined with Student's *t* test. Statistical differences among more than three groups were determined using a one-way ANOVA, two-way ANOVA, or an ANOVA with repeated measures (two or three-factor), followed by the Bonferroni's multiple comparison test (Bonferroni's correction; 3, 6, 15, and 36 comparisons in 3, 4, 6, and 9 groups, respectively). $p < 0.05$ was regarded as statistically significant.

Nucleotide sequences. The DNA Data Bank of Japan/GenBank/European Molecular Biology Laboratory accession number for the primary nucleotide sequence of shati is DQ174094.

Results

Identification of shati

The reasons why we pursued shati for intensive investigation arose from our preliminary findings with the PCR-select cDNA subtraction method to detect the genes in the NAc affected by METH treatment: mice were administrated METH (2 mg/kg, s.c.) or saline for 6 d, and shati mRNA production in the NAc was found to increase by 640% in METH-treated mice with robust behavioral sensitization compared with saline-treated mice (data not shown). The sequence of cDNA was completely matched to accession number NM_001001985 of NCBI gene bank (the gene

record was replaced by accession number NM_001001985.2 on April, 10, 2005). The sequence has been identified by the Mammalian Gene Collection Program Team (Strausberg et al., 2002). Blackshaw et al. (2004) has demonstrated the extended cDNA sequence by serial analysis of gene expression methods, which provides an unbiased and nearly comprehensive readout of gene expression and that the gene was for one of the proteins related to the retina development. We named this novel molecule shati after the symbol at Nagoya castle in Japan. The sequence is translated to a protein LOC269642 (accession number is NP_001001985.1 and 2; 001001985.1 was a part of 001001985.2) (supplemental Fig. 1, available at www.jneurosci.org as supplemental material).

Characterization of shati

Homology modeling for C-terminal domain of shati was established using MOE software (Chemical Computing Group) (Fig. 1*A*,*B*). Red character in Figure 1*A* showed homology modeling of shati. From motif analysis of shati, shati contained the sequence of GCN5-related *N*-acetyltransferase (GCAT) (Fig. 1*C*). Underlined character in Figure 1*A* showed GNAT motif. Docking simulations of acetyl-CoA or ATP with shati protein were also examined using MOE software (Chemical Computing Group) to calculate the interactive potential energy of molecules. Shati also contained acetyl-CoA binding or ATP binding site, because the analysis showed the lowest interactive potential energy of shati with acetyl-CoA or ATP, −301 and −322 kcal, respectively (supplemental Fig. 2, available at www.jneurosci.org as supplemental material). Docking simulations of shati with DA, DNA binding site, and nuclear localization signals showed too high interactive potential energy of molecules or no domain.

Expression of shati mRNA

As shown in Figure 2*A*, RT-PCR analysis revealed that shati is expressed at high levels in the cerebrum, cerebellum, liver, kidney, and spleen. We amplified and analyzed its three different target sequences by RT-PCR (Table 1). Similar results of RT-PCR were obtained with three different sets of primers (Fig. 2*A*).

We performed a series of experiments to validate the results of cDNA subtraction. Repeated METH treatment (2 mg/kg, s.c.) for 6 d significantly elevated the mRNA levels of the target sequences of shati in the NAc (Fig. 2*B*).

METH-induced expression of shati mRNA in the brain

As an initial step in assessing the relationship between shati and METH-induced sensitization and dependence, we examined whether single and repeated METH treatment altered the expression of shati mRNA in the mouse brain using the real-time RT-PCR method. The effects of repeated METH treatment (0.3, 1 and 2 mg/kg, s.c. for 3 d) on shati mRNA expression in the NAc were dose dependent ($F_{(3,28)} = 5.503$; $p < 0.01$, one-way ANOVA) (Fig. 3*A*). The levels of shati mRNA were significantly increased 2, 6, and 24 h after the last METH treatment and then returned to control value 1 week after the treatment ($F_{(6,41)} = 4.444$; $p < 0.01$, one-way ANOVA) (Fig. 3*B*). Single METH treatment (2 mg/kg, s.c.) remarkably induced shati mRNA expression in the NAc and hippocampus (Hip). METH (2 mg/kg, s.c.) or saline challenge on day 6 after repeated administration of METH (2 mg/kg, s.c.) for 5 d remarkably induced shati mRNA expression in the frontal cortex (Fc), NAc, and caudate–putamen (CPu) (repeated drug administration, $F_{(1,32)} = 20.368$, $p < 0.01$ for Fc; single administration, $F_{(1,32)} = 0.005$, $p = 0.942$ for Fc; repeated drug administration × single administration, $F_{(1,32)} = 1.643$, $p = 0.209$ for Fc; repeated drug administration, $F_{(1,31)} = 14.436$, $p <$

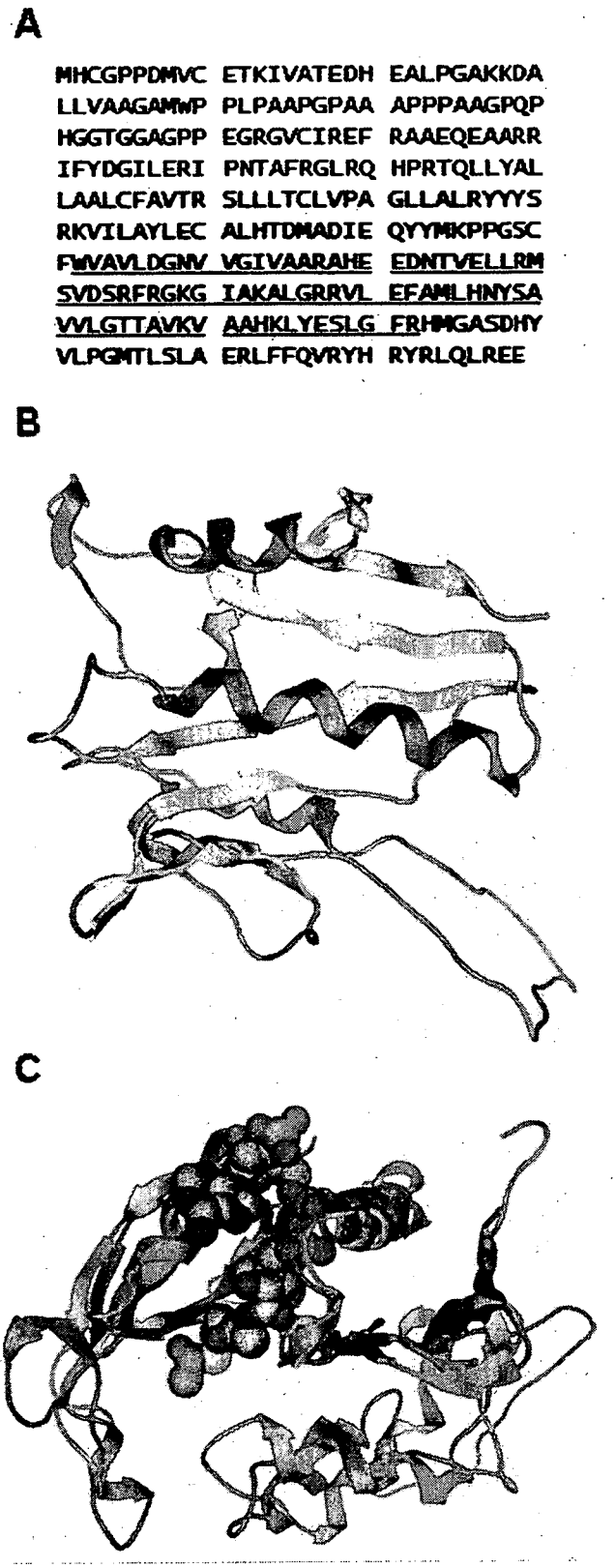

Figure 1. Characterization of shati. *A*, The sequence of shati. The red character showed homology modeling of shati. The underlined character showed GCN5-related *N*-acetyltransferase motif. *B*, Homology modeling for C-terminal domain of shati. *C*, Homology modeling and motif analysis of shati. Shati has the sequence of GCAT. Red ribbon, Homology model of shati; sphere, acetyl-CoA analyzed by x-ray crystallography; green ribbon, *N*-acetyltransferase.

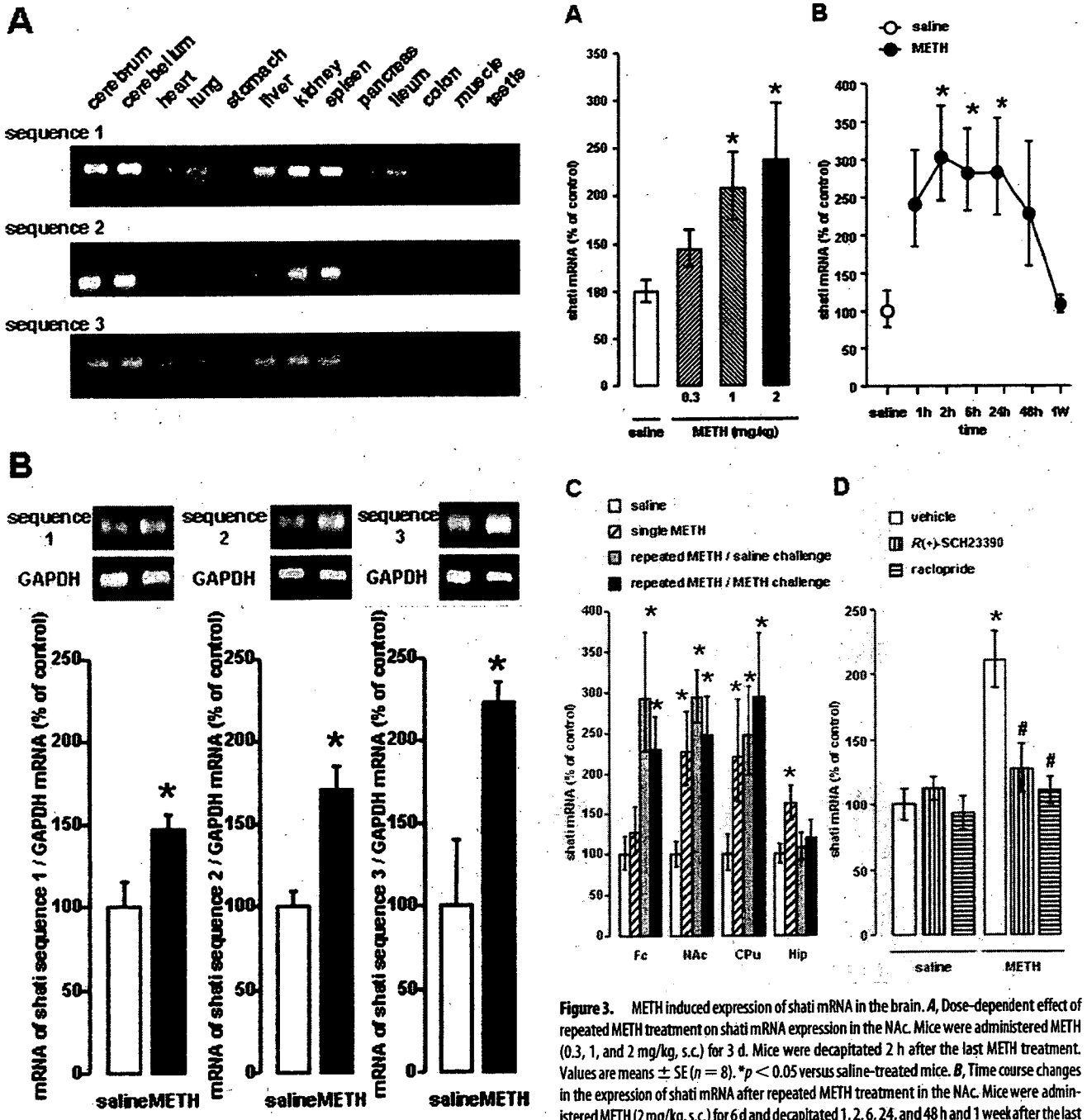

Figure 2. Expression of shati mRNA in the various organs of mice. *A*, RT-PCR analysis of shati in the various organs in mice. Mice were decapitated without any treatment, and the brains were quickly removed. The sets of primers used for PCR are listed in Table 1. *B*, Increase in the production of the three sets of target sequences of shati induced by repeated METH treatment in the NAc of mice. Mice were administered METH (2 mg/kg, s.c.) for 6 d and decapitated 2 h after the last METH treatment. Values are means ± SE ($n = 5$). *$p < 0.05$ versus saline-treated mice. To standardize the PCR products, we used primers for glyceraldehyde-3-phosphate dehydrogenase (GAPDH) as the internal control.

Figure 3. METH induced expression of shati mRNA in the brain. *A*, Dose-dependent effect of repeated METH treatment on shati mRNA expression in the NAc. Mice were administered METH (0.3, 1, and 2 mg/kg, s.c.) for 3 d. Mice were decapitated 2 h after the last METH treatment. Values are means ± SE ($n = 8$). *$p < 0.05$ versus saline-treated mice. *B*, Time course changes in the expression of shati mRNA after repeated METH treatment in the NAc. Mice were administered METH (2 mg/kg, s.c.) for 6 d and decapitated 1, 2, 6, 24, and 48 h and 1 week after the last METH treatment. Values are means ± SE ($n = 6–7$). *$p < 0.05$ versus saline-treated mice. *C*, Changes in the expression of shati mRNA in the various brain regions (Fc, NAc, CPu, and Hip) of the mice after single and repeated METH treatment. Mice were administered METH (2 mg/kg, s.c.) for 5 d and challenged with METH (2 mg/kg, s.c.) or saline on day 6. Mice were decapitated 2 h after last treatment of METH (2 mg/kg, s.c.) or saline challenge. Values are means ± SE ($n = 8–10$). *$p < 0.05$ versus saline-treated mice. *D*, The effects of the DA D_1-like receptor antagonist *R*(+)-SCH23390 or D_2-like receptor antagonist raclopride on METH-induced expression of shati mRNA in the NAc. Mice were treated with *R*(+)-SCH23390 (0.1 mg/kg, s.c.) or raclopride (2 mg/kg, s.c.) 30 min before daily METH (2 mg/kg, s.c. for 6 d) treatment. Mice were decapitated 2 h after the last METH treatment. Values are means ± SE ($n = 6–8$). *$p < 0.05$ versus vehicle/saline-treated mice. #$p < 0.05$ versus vehicle/METH-treated mice.

0.01 for NAc; single administration, $F_{(1,31)} = 4.917$, $p < 0.05$ for NAc; repeated drug administration × single administration, $F_{(1,31)} = 10.545$, $p < 0.01$ for NAc; repeated drug administration $F_{(1,32)} = 8.023$, $p < 0.01$ for CPu; single administration, $F_{(1,32)} = 4.833$, $p < 0.05$ for CPu; repeated drug administration × single administration, $F_{(1,32)} = 1.669$, $p = 0.206$ for CPu; repeated drug administration, $F_{(1,32)} = 0.628$, $p = 0.434$ for Hip; single administration, $F_{(1,32)} = 6.464$, $p < 0.05$ for Hip; repeated drug administration × single administration, $F_{(1,32)} = 2.496$, $p = 0.124$ for Hip; two-way ANOVA) (Fig. 3*C*). The increase caused by METH in the NAc was inhibited by pretreatment with either the DA

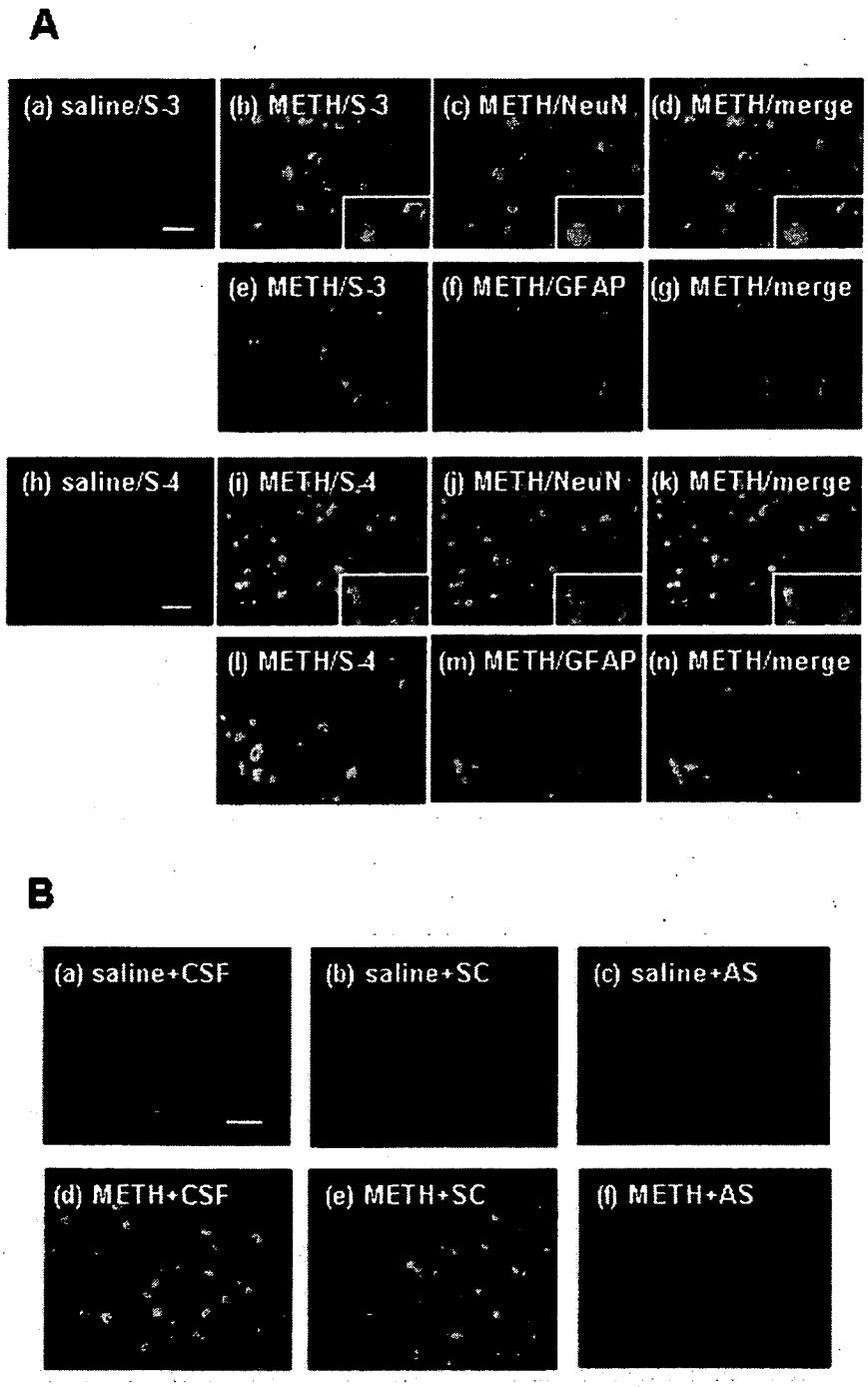

Figure 4. Immunostaining of shati in the NAc after repeated treatment with METH. Mice were administered METH (2 mg/kg, s.c.) for 6 d and decapitated 24 h after the last treatment. *A*, Double-labeling fluorescence photomicrographs for shati and NeuN or GFAP. The shati-immunopositive cells (green) were colocalized with NeuN-immonopositive cells (red). Double immunostaining for S-3 or S-4 and NeuN in the NAc reveals shati expression in neuronal cells. Scale bars, 20 μm. *B*, Effect of shati-AS on METH-induced increase in shati expression. METH-induced increase in shati expression in the NAc was inhibited by shati-AS. Scale bar, 20 μm.

D_1-like receptor antagonist *R*(+)-SCH23390 (0.1 mg/kg, i.p.) or the D_2-like receptor antagonist raclopride (2 mg/kg, i.p.) (agonist, $F_{(1,34)} = 18.649$, $p < 0.01$; antagonist, $F_{(2,34)} = 5.554$, $p < 0.01$; agonist × antagonist, $F_{(2,34)} = 5.382$, $p < 0.01$; two-way ANOVA) (Fig. 3*D*), although neither antagonists had an effect on shati mRNA expression in the saline-treated mice. These results indicate that METH induces the expression of shati mRNA in the brain through the activation of both DA D_1 and D_2 receptors.

Localization of shati in the brain of mice treated with METH

There were few shati-immunopositive cells in saline-treated mouse brain (Fig. 4*Aa*,*Ah*). METH (2 mg/kg, s.c. for 6 d) increased the number of shati-immunopositive cells in the NAc compared with that in saline-treated mice (Fig. 4*A*). The shati-immunopositive cells were diminished when the antibodies were absorbed by S-3 or S-4 antigen (data not shown). The shati-immunopositive cells were colocalized with the cells that were immunopositive for NeuN, a neuronal marker, but not for GFAP, an astroglial marker, in the NAc of mice (Fig. 4*Ab–Ag*,*Ai–An*). The repeated METH treatment-induced increase in the numbers of shati-immunopositive cells in the NAc was abolished by shati-AS treatment, although shati-SC had no effect (Fig. 4*Ba–Bf*).

Roles of shati in METH-induced hyperlocomotion and sensitization

To examine the role of shati in the behavioral and neurochemical phenotype in response to METH, we used an AS strategy, which widely used to manipulate gene expression in the brain via intracerebroventricular infusion (Taubenfeld et al., 2001; Bowers et al., 2004). The experimental schedules are shown in Figure 5, *A* and *C*. The AS downregulated the expression of shati mRNA in the NAc (Fig. 5*B*). The increase in the levels of shati mRNA expression evoked by repeated METH treatment in the NAc was significantly and completely abolished by shati-AS, although shati-SC had no effect. Moreover, shati mRNA expression in the NAc of saline-treated mice was also reduced by shati-AS, whereas shati-SC did not affect the expression in saline-treated mice (drug, $F_{(1,42)} = 72.765$, $p < 0.01$; intracerebroventricular treatment, $F_{(2,42)} = 14.104$, $p < 0.01$; drug × intracerebroventricular treatment, $F_{(2,42)} = 0.092$, $p = 0.912$; two-way ANOVA) (Fig. 5*B*), indicating that shati-AS has an ability to reduce effectively the expression of shati mRNA. We also examined the effect of shati-AS on tPA expression as one of drug-dependence-related other proteins, because tPA–plasmin system potentiates the rewarding and locomotor-stimulating effects of METH, MOR, and nicotine by regulating release of DA (Nagai et al., 2004, 2005a,b, 2006). The increase in the levels of tPA mRNA expression in the NAc was not abolished by shati-AS (drug, $F_{(1,47)} = 62.530$, $p < 0.01$; intracerebroventricular treatment, $F_{(2,47)} = 0.148$, $p = 0.862$; drug × intracerebroventricular treatment, $F_{(2,47)} = 0.803$, $p = 0.454$; two-way ANOVA). Moreover, tPA mRNA expression in the NAc of saline-treated mice was not also reduced by shati-AS, indicating that shati-AS has no ability to

reduce effectively the expression of tPA mRNA (data not shown). Therefore, shati-AS is considered to have no secondary effects.

Repeated METH administration leads to a progressive augmentation of many behavioral effects of the drug (behavioral sensitization). Sensitization is of interest as a model for drug-induced neuroplasticity in neuronal circuits important for addiction. It is well established that the induction of sensitization involves complex neuronal circuitry (Wolf, 1998). In rodent, sensitization is observed as a progressive augmentation of locomotor activity that may relate to an increase in the incentive to obtain drugs (Robinson and Berridge, 1993; Lorrain et al., 2000). There is also evidence of sensitization in human drug users (Satel et al., 1991) and normal subjects (Strakowski and Sax, 1998). Repeated METH treatment (1 and 2 mg/kg, s.c.) for 5 d produced behavioral sensitization [$F_{(2,12)} = 7.404$ for METH (1 mg/kg) plus shati-AS-treated mice; $F_{(2,18)} = 5.593$ for METH (1 mg/kg) plus shati-SC-treated mice; $F_{(2,18)} = 30.917$ for METH (1 mg/kg) plus CSF-treated mice; $F_{(2,12)} = 7.453$ for METH (2 mg/kg) plus shati-AS-treated mice, $F_{(2,12)} = 4.243$ for METH (2 mg/kg) plus shati-SC-treated mice; $F_{(2,15)} = 8.569$ for METH (2 mg/kg) plus CSF-treated mice; $p < 0.05$, one-way ANOVA] (Fig. 5*D*). As shown in Figure 5*D*, the shati-AS treatment potentiated the METH (1 mg/kg, s.c.)-induced hyperlocomotion and sensitization compared with shati-SC- or CSF-treated mice (drug, $F_{(2,141)} = 291.696$, $p < 0.01$; intracerebroventricular treatment, $F_{(2,141)} = 28.223$, $p < 0.01$; time, $F_{(2,141)} = 17.154$, $p < 0.01$; drug × intracerebroventricular treatment, $F_{(4,141)} = 12.432$, $p < 0.01$; drug × time, $F_{(4,141)} = 12.913$, $p < 0.01$; intracerebroventricular treatment × time, $F_{(4,141)} = 0.156$, $p = 0.960$; drug × intracerebroventricular treatment × time, $F_{(8,141)} = 0.427$, $p = 0.903$; three-factor repeated ANOVA), whereas the shati-AS, shati-SC, or CSF treatment had no effect on spontaneous locomotor activity (Fig. 5*D*). The sensitization was observed on day 10 after challenge administration of METH (0.3 mg/kg, s.c.). Shati-AS-treated mice showed a marked potentiation of METH (0.3 mg/kg, s.c.)-induced sensitization on day 10 compared with shati-SC- or CSF-treated mice ($F_{(2,13)} = 6.974$, $p < 0.05$, one-way ANOVA), although shati-AS-treated mice did not show a potentiation of METH (2 mg/kg, s.c.)-induced hyperlocomotion and sensitization compared with shati-SC- or CSF-treated mice on days 1–5 (Fig. 5*D*).

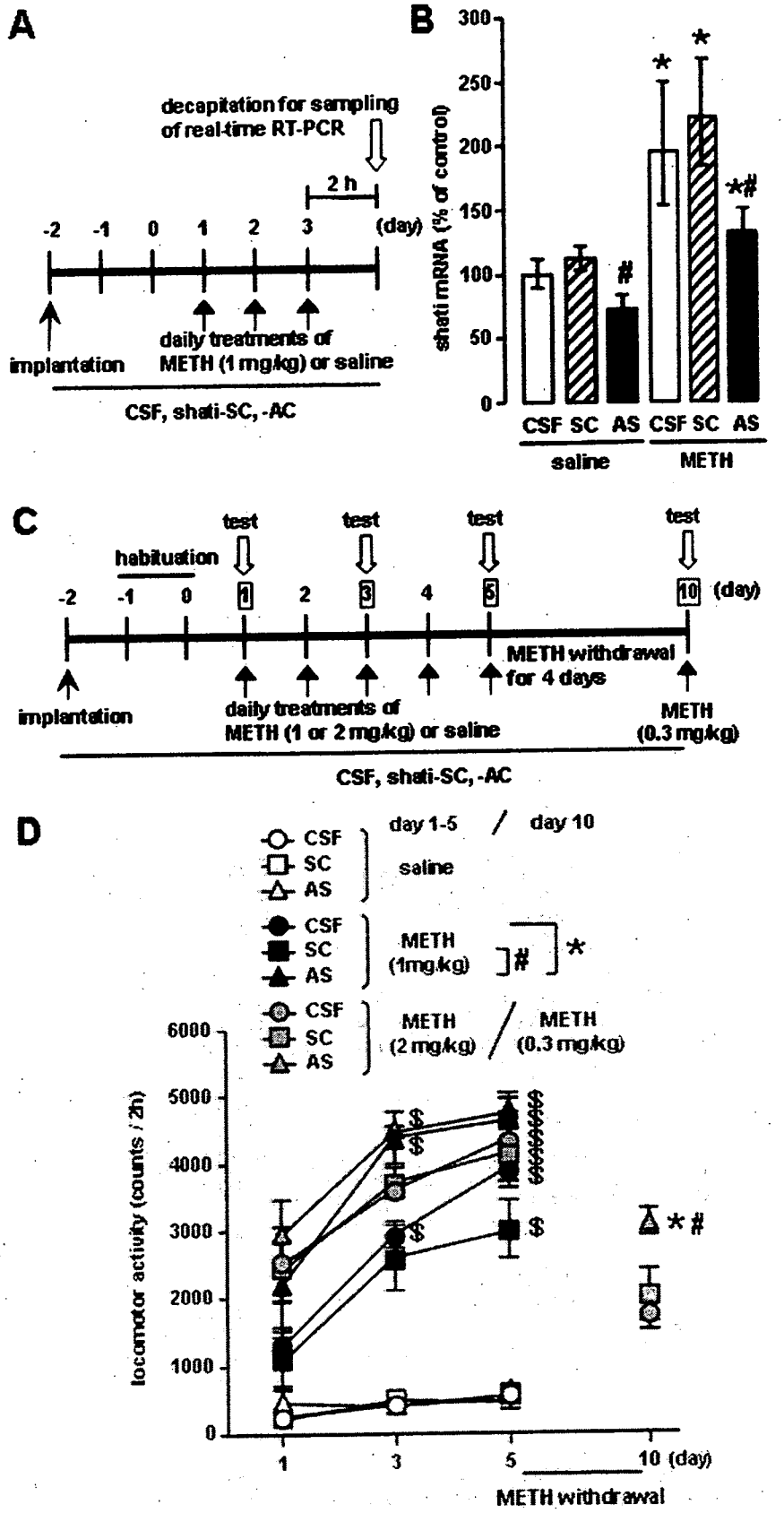

Figure 5. Roles of shati in METH-induced hyperlocomotion and sensitization. An osmotic minipump was used to deliver a continuous infusion of shati-AS (1.8 nmol/6 μl per day), shati-SC (1.8 nmol/6 μl per day), or CSF into the right ventricle (AP −0.5 mm, ML +1.0 mm from bregma, and DV −2.0 mm from the skull). *A*, Experimental schedule for the real-time RT-PCR using shati-AS. *B*, Effect of shati-AS on shati mRNA expression. Mice were administered METH (1 mg/kg, s.c.) for 3 d and decapitated 2 h

Roles of shati in METH-induced dopaminergic responses

The pharmacological effects of METH are linked to its capacity to elevate extracellular DA levels by releasing DA from presynaptic nerve terminals and inhibiting its reuptake (Heikkila et al., 1975; Seiden et al., 1993). In addition, METH and the amphetamines redistribute DA from synaptic vesicles to the cytosol and promote reverse transport (Seiden et al., 1993). Therefore, we examined the effect of shati-AS on the METH-induced increase in overflow of DA in the NAc using an *in vivo* microdialysis technique. The experimental schedule is shown in Figure 6*A*. METH caused a marked increase in overflow of DA in the NAc of the CSF-treated mice on the day 3 (Fig. 6*B*). The peak of overflow of DA was increased by METH treatment to ~360% of the baseline level in the CSF-treated mice. In shati-AS-treated mice, the METH-induced increase in overflow of DA was significantly potentiated compared with that in the shati-SC- or CSF-treated mice (intracerebroventricular treatment, $F_{(2,14)} = 5.662$, $p < 0.05$; time, $F_{(10,140)} = 35.646$, $p < 0.01$; intracerebroventricular treatment × time, $F_{(20,140)} = 1.927$, $p < 0.05$; repeated ANOVA) (Fig. 6*B*). The levels of basal DA did not differ among the three groups.

Next, we examined the *in vivo* effect of shati-AS on [^{3}H]DA uptake into synaptosomes in the midbrain. The experimental schedule is shown in Figure 6*C*. METH decreased [^{3}H]DA uptake compared with the saline-treated mice. In shati-AS-treated mice, the METH-induced decrease in [^{3}H]DA uptake was significantly potentiated compared with that in the shati-SC- or CSF-treated mice. Moreover, [^{3}H]DA uptake in the saline-treated group was also decreased by shati-AS compared with that in the shati-SC- or CSF-treated mice, although shati-SC had no effect on [^{3}H]DA uptake (drug, $F_{(1,40)} = 30.447$, $p < 0.01$; intracerebroventricular treatment, $F_{(2,40)} = 12.576$, $p < 0.01$; drug × intracerebroventricular treatment, $F_{(2,40)} = 0.392$, $p = 0.678$; two-way ANOVA) (Fig. 6*D*).

We also examined the *in vivo* effect of shati-AS on [^{3}H]DA uptake into synaptic vesicle preparations in the midbrain, because the redistribution of DA from synaptic vesicles to cytoplasmic compartments through interaction with vesicular monoamine transporter-2 has been postulated to be primarily responsible for DA terminal injury by METH or amphetamines (Liu and Edwards, 1997; Uhl, 1998). METH decreased vesicular [^{3}H]DA uptake compared with the saline-treated mice. In shati-AS-treated mice, the METH-induced decrease in vesicular [^{3}H]DA uptake was significantly potentiated compared with that in the shati-SC- or CSF-treated mice. Moreover, [^{3}H]DA uptake in the saline-treated group was also decreased by shati-AS compared with that in the shati-SC- or CSF-treated mice, although shati-SC had no effect on [^{3}H]DA uptake (drug, $F_{(1,42)} = 137.229$, $p < 0.01$; intracerebroventricular treatment, $F_{(2,42)} = 15.087$, $p < 0.01$; drug × intracerebroventricular treatment, $F_{(2,42)} = 0.240$, $p = 0.788$; two-way ANOVA) (Fig. 6*E*).

Different results were obtained from *in vivo* microdialysis and DA uptake studies, only in the basal conditions. These studies were performed in quite different situations. Living mice were used *in vivo* microdialysis study, and basal overflow of endogenous DA was measured 24 h after the last METH treatment in the NAc (Fig. 6*B*). Therefore, other factors (other neurotransmitters, neuroplasticity, and neuronal input from other brain regions) might affect basal DA overflow and compensate the dysfunction of DA uptake induced by repeated treatment of METH. Conversely, the experiment of [^{3}H]DA uptake was *ex vivo* study by using the midbrain tissue (Fig. 6*D*,*E*). High-concentration and exogenous [^{3}H]DA was used for the investigation of functional changes of DA uptake 1 h after the last METH treatment in the midbrain. The *ex vivo* method could more directly measure the changes of DA uptake in the midbrain, comparing *in vivo* microdialysis study.

Roles of shati in METH-induced conditioned place preference

The effect of shati-AS on METH-induced CPP was examined in a place conditioning paradigm, in which animals learn the association of an environment paired with drug exposure. This paradigm involves sensory perception of external stimuli, association of stimuli, and the approach-inducing actions of a drug, as well as the rewarding effects of a drug. The experimental schedule is shown in Figure 7*A*. As shown in Figure 7*B*, METH (0.3 mg/kg, s.c.) produced place preference in mice. In shati-AS-treated mice, the development of METH-induced CPP was significantly potentiated compared with that in the shati-SC- or CSF-treated mice (drug, $F_{(1,46)} = 78.202$, $p < 0.01$; intracerebroventricular treatment, $F_{(2,46)} = 4.950$, $p = 0.011$; drug × intracerebroventricular treatment, $F_{(2,46)} = 5.046$, $p = 0.010$; two-way ANOVA) (Fig. 7*B*), indicating that downregulation of shati expression was sufficient to confer the enhanced METH-induced CPP. Shati-AS, shati-SC, or CSF treatment had no effect on CPP in saline-treated mice (Fig. 7*B*, left three columns), suggesting that the procedure in CPP might not reflect anxiolytic actions. These results suggest that shati participates in the repeated METH treatment-induced development of behavioral sensitization and CPP by regulating DA uptake.

Discussion

In the present study, we identified a novel molecule shati from the NAc of mice treated with METH for the first time using the PCR-select cDNA subtraction method, which is a differential and epochal cloning technique.

From motif analysis of shati, shati contained the sequence of GCAT (Fig. 1*C*). Shati might have physiological action in producing acetylcholine or metabolic action of ATP, because the analysis showed the lowest interactive potential energy of shati with acetyl-CoA or ATP (supplemental Fig. 2, available at www.jneurosci.org as supplemental material). Accordingly, we have to investigate the mechanism by which shati regulates production of acetylcholine or metabolic roles of ATP in subsequent studies.

Because shati expression was detected at high levels in not only the brain regions related to drug dependence but also the liver, kidney, and spleen (Fig. 2*A*), it is plausible that shati is involved in the regulation of pathophysiological function. Single METH treatment induced the expression of shati mRNA in the NAc and Hip (Fig. 3*C*). Repeated METH treatment produces an enhancement of the locomotor-stimulating effects of METH (data not shown). Remarkable induction of shati mRNA expression was detected in the Fc, NAc, and CPu of the mice that

←

after METH treatment on the day 3. Values are means ± SE ($n = 8$). *$p < 0.05$ versus saline-treated mice. #$p < 0.05$ versus shati-SC-treated mice. *C*, Experimental schedule for measurement of locomotor activity using shati-AS. *D*, Effect of shati-AS on repeated METH-induced behavioral sensitization. Mice were administered METH (1 or 2 mg/kg, s.c.) or saline for 5 d and challenged with METH (0.3 mg/kg, s.c.) on day 10. Locomotor activity was measured for 2 h on the days 1, 3, 5, and 10. Values are means ± SE ($n = 5$–7). ANOVA with repeated measures revealed significant differences in METH-induced sensitization (group, $F_{(8,47)} = 51.238$, $p < 0.01$; day, $F_{(2,94)} = 68.423$, $p < 0.01$; group × day, $F_{(16,94)} = 4.412$, $p < 0.01$). *$p < 0.05$ versus METH plus CSF-treated mice. #$p < 0.05$ versus METH plus shati-SC-treated mice. $$p < 0.05$ versus the locomotor activity on day 1 in the same group.

showed behavioral sensitization to METH (Fig. 3*A–C*). There is strong evidence that the dopaminergic system, which projects from the VTA of the midbrain to the NAc and to other forebrain sites, including the Fc, dorsal striatum, and Hip, is a major substrate of reward and reinforcement for both natural rewards and addictive drugs (Di Chiara and Imperato, 1988; Robbins and Everitt, 1996; Wise, 1996a). Therefore, shati may be involved in the rewarding effects and reinforcement of addictive drugs. Because the dopaminergic neuronal system is involved primarily in the pharmacological effects of METH (Melega et al., 1995; Larsen et al., 2002; Sulzer et al., 2005), we examined whether the METH-induced increase in shati mRNA levels is mediated by the activation of dopaminergic neurotransmission. The METH-induced increase in the expression of shati mRNA in the NAc was completely inhibited by pretreatment with the DA D_1-like receptor antagonist *R*(+)-SCH23390 and the DA D_2-like receptor antagonist raclopride (Fig. 3*D*), suggesting that the activation of DA D_1 and D_2 receptors is attributable to METH-induced expression of shati. Behavioral studies have suggested that both DA D_1 and D_2 receptors mediate reinforcing signals for drug of abuse, because amphetamine-induced CPP and METH-induced sensitization are blocked by either DA D_1-like or D_2-like receptor antagonist (Ujike et al., 1989; Hiroi and White, 1991). Therefore, it likely that activation of DA transmission is necessary for METH-induced shati expression in neurons, in which shati specifically acts (Fig. 4*A*).

The contribution of dopaminergic transmission to behavioral sensitization and CPP has been well documented (Nakajima et al., 2004; Nagai et al., 2005a,b; Niwa et al., 2007a,b,d). Shati expression was upregulated by repeated administration of METH (Figs. 2*B*, 3, 4*A*), and downregulation of shati by AS (Figs. 4*B*, 5*B*) led to an elevated synaptic DA concentration in the NAc and major behavioral manifestations in mice: heightened locomotor activity (Fig. 5*D*), the rate of development of sensitization (Fig. 5*D*), and CPP (Fig. 7*B*) responding to METH. Furthermore, downregulation of shati expression by AS (Figs. 4*B*, 5*B*) potentiated the effects of METH on overflow of DA in the NAc (Fig. 6*B*) and DA uptake (Fig. 6*D*,*E*). These findings strongly suggest that the overexpression of shati elicited by METH may serve as a homeostatic mechanism that prevents hyperlocomo-

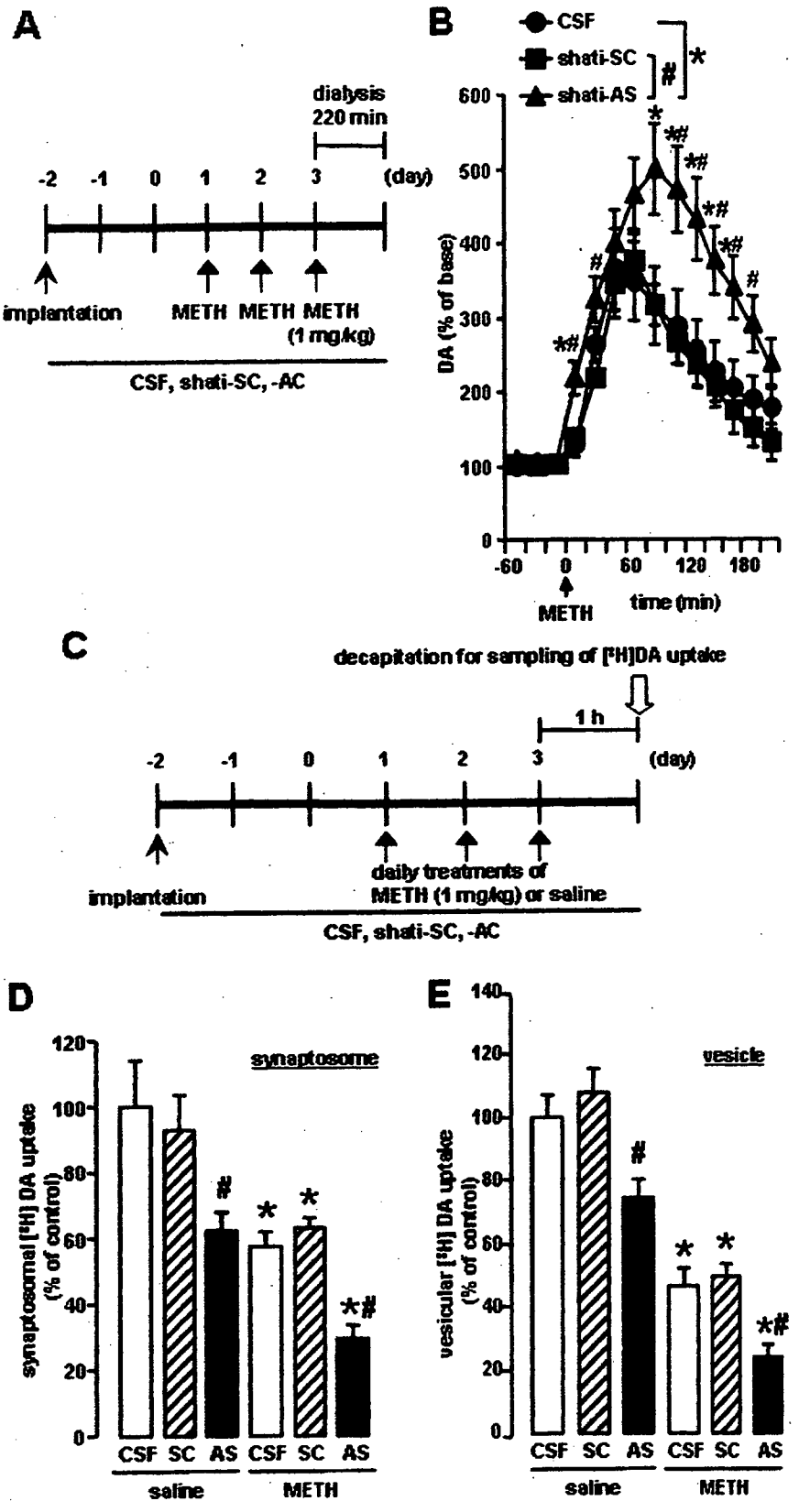

Figure 6. Effects of shati-AS on METH-induced dopaminergic responses. *A*, Experimental schedule for the measurement of overflow of DA using *in vivo* microdialysis using shati-AS. *B*, Effect of shati-AS on METH-induced increase in overflow of DA in the NAc. Mice were administered METH (1 mg/kg, s.c.) for 3 d. On day 3, levels of DA were measured in the NAc (AP +1.7 mm, ML −0.8 mm from bregma, and DV −4.0 mm from the skull) for 220 min after METH treatment by *in vivo* microdialysis. Basal levels of DA were 0.30 ± 0.08, 0.31 ± 0.05, and 0.30 ± 0.04 nM for the CSF-treated, shati-SC-treated, and shati-AS-treated mice, respectively. ANOVA with repeated measures revealed significant differences in METH-induced increase in overflow of DA (group,

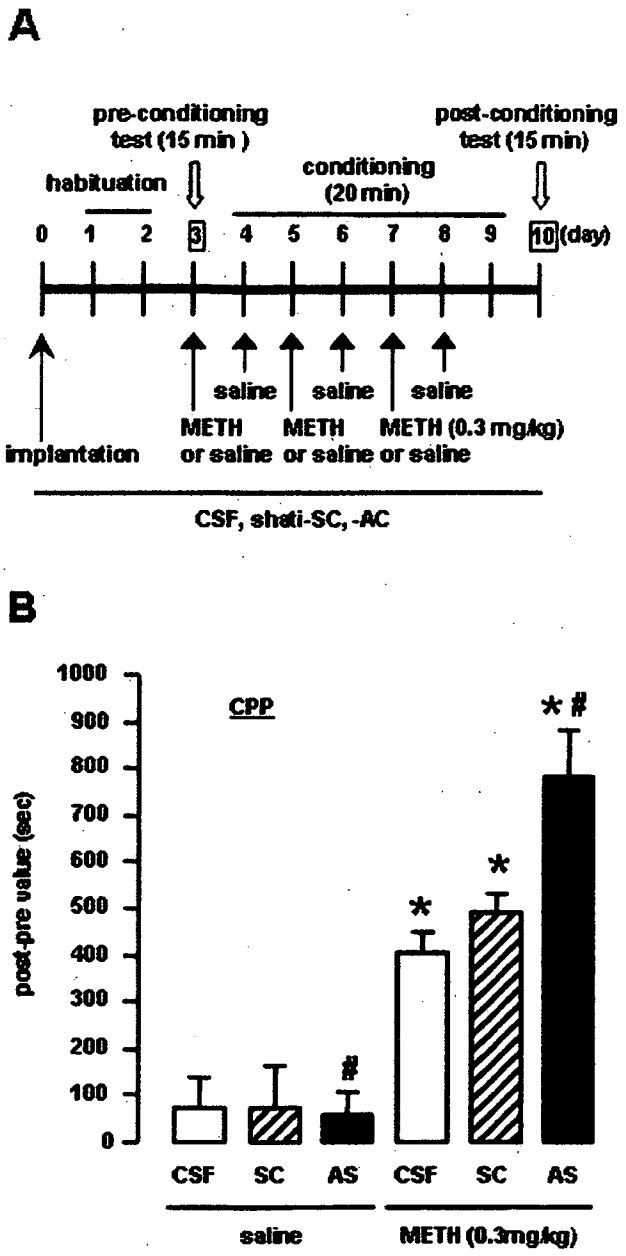

Figure 7. Effects of shati-AS on METH-induced conditioned place preference. *A*, Experimental schedule for the conditioned place preference task using shati-AS. *B*, Effect of shati-AS on METH-induced place preference. Mice were administered METH (0.3 mg/kg, s.c.) or saline during the conditioning for place preference. Values are means ± SE ($n = 5–12$). *$p < 0.05$ versus saline-treated mice. #$p < 0.05$ versus shati-SC-treated mice.

←

$F_{(2,14)} = 5.662, p < 0.05$; time, $F_{(10,140)} = 35.646, p < 0.01$; group × time, $F_{(20,140)} = 1.927, p < 0.05$). Values are means ± SE ($n = 5–6$). *$p < 0.05$ versus CSF-treated mice. #$p < 0.05$ versus shati-SC-treated mice. *C*, Experimental schedule for the [^{3}H]DA uptake assay using shati-AS. *D*, Effect of shati-AS on METH-induced decrease of synaptosomal [^{3}H]DA uptake. Mice were administered METH (1 mg/kg, s.c.) for 3 d and decapitated 1 h after the last injection. The synaptosomal [^{3}H]DA uptake was 0.32 ± 0.04, 0.29 ± 0.03, 0.20 ± 0.02, 0.18 ± 0.01, 0.20 ± 0.01, and 0.09 ± 0.01 pmol/mg protein per 4 min for the saline plus CSF-treated, saline plus shati-SC-treated, saline plus shati-AS-treated, METH plus CSF-treated, METH plus shati-SC-treated, and METH plus shati-AS-treated mice, respectively. The final concentration of [^{3}H]DA was 5 nM. Values are means ± SE ($n = 7–8$). *$p < 0.05$ versus saline-treated mice. #$p < 0.05$ versus shati-SC-treated mice. *E*, Effect of shati-AS on METH-induced decrease of vesicular [^{3}H]DA uptake. Mice were administered METH (1 mg/kg, s.c.) for 3 d and decapitated 1 h after the last injection. The vesicular [^{3}H]DA uptake was 3.76 ± 0.25, 4.05 ± 0.29, 2.80 ± 0.20, 1.74 ± 0.21, 1.85 ± 0.14, and 0.90 ± 0.14 pmol/mg protein per 4 min for the saline plus CSF-treated, saline plus shati-SC-treated, saline plus shati-AS-treated, METH plus CSF-treated, METH plus shati-SC-treated, and METH plus shati-AS-treated mice, respectively. The final concentration of [^{3}H]DA was 30 nM. Values are means ± SE ($n = 8$). *$p < 0.05$ versus saline-treated mice. #$p < 0.05$ versus shati-SC-treated mice.

tion, sensitization, and CPP, by promoting plasmalemmal and vesicular DA uptake as well as attenuating the METH-induced increase in overflow of DA in the NAc.

We used METH at the dose of 2 mg/kg for 6 d in the experiments of RT-PCR, real-time RT-PCR, and immunohistochemistry (Figs. 3, 4*B–D*, 5), because expression of shati was induced in the NAc of mice by METH (2 mg/kg for 6 d), which was detected by using a PCR-select cDNA subtraction method (supplemental Fig. 1, available at www.jneurosci.org as supplemental material). In AS experiments, shati-AS-treated mice tended to show a potentiation of METH (2 mg/kg)-induced hyperlocomotion and sensitization on days 1–5, but there were no statistically significant differences among the three groups (Fig. 5*D*). The dose–response effects of METH on the locomotor activity may reflect a shift to the left, but these effects were reached the plateau. Conversely, shati-AS-treated mice showed a marked potentiation of METH (1 mg/kg)-induced hyperlocomotion and sensitization on days 1–5 compared with shati-SC- or CSF-treated mice (Fig. 5*D*). On day 3, the potentiation of the METH-induced hyperlocomotion by shati-AS reached the maximum and plateau. Therefore, in the experiments of AS, we selected METH at the dose of 1 mg/kg for 3 d (Figs. 5*B*, 6*B,D,E*). We also confirmed that shati mRNA was increased by METH at the doses of 1 and 2 mg/kg for 3 d (Fig. 3*A*). Then, in the AS study, we selected METH at the dose of 1 mg/kg to investigate effects of AS.

We selected the time point of 2 h after the last METH treatment for the time when the animals were to be killed in the experiments of RT-PCR and real-time RT-PCR (Figs. 2, 3*A,C,D*), because expression of shati mRNA showed peak in the NAc of mice 2 h after the last METH treatment (Fig. 3*B*). We prepared the brain samples 24 h after the last METH treatment for immunohistochemical study (Fig. 4). The levels of shati mRNA in the NAc of mice treated with repeated METH were significantly increased 2, 6, and 24 h after the last METH treatment (Fig. 3*B*). At 24 h after the METH treatment, both transcription and translation of shati protein could be induced in the brain. Therefore, we considered that 24 h after the METH treatment is the best time point for investigation of shati protein expression.

Changes in mRNA and protein expression caused by drugs are of particular interest. The expression of certain mRNAs and proteins appears to be a compensatory adaptation to excessive DA signaling, which could be biologically significant adaptive mechanisms contributing to dependence. Nevertheless, some proteins play a reverse role. For example, we previously demonstrated that tPA potentiates METH- or MOR-induced rewarding and locomotor-stimulating effects (Nagai et al., 2004, 2005a,b), whereas TNF-α and its inducer inhibit them (Nakajima et al., 2004; Niwa et al., 2007a,b,d). The development of sensitization to amphetamine is prevented when an antibody that neutralized basic fibroblast growth factor (bFGF) is infused into the VTA before amphetamine treatment (Flores et al., 2000). Infusion of brain-derived neurotrophic factor (BDNF) into the NAc enhances the stimulation of locomotor activity by cocaine in rats, whereas the development of sensitization and CPP is delayed in heterozygous BDNF knock-out mice compared with wild-type littermates (Horger et al., 1999; Hall et al., 2003). Infusion of GDNF into the VTA blocks certain biochemical adap-

tations to chronic cocaine treatment (induction of tyrosine hydroxylase, NR1 subunit of NMDA receptors, ΔFosB, and protein kinase A catalytic subunit) as well as cocaine-induced rewarding effects (Messer et al., 2000). Conversely, responses to cocaine are enhanced in rats by intra-VTA infusion of anti-GDNF antibody and in GDNF heterozygous knock-out mice (Messer et al., 2000). A partial reduction in the expression of GDNF potentiates METH self-administration, enhances motivation to take METH, increases vulnerability to drug-primed reinforcement, and prolongs cue-induced reinforcement of extinguished METH-seeking behavior (Yan et al., 2007). cAMP response element-binding protein (CREB) overexpression in the NAc reduces the rewarding properties of cocaine, whereas expression of a dominant-negative form of CREB in this region has the opposite effect (Carlezon et al., 1998; Walters and Blendy, 2001; McClung and Nestler, 2003). Furthermore, *Fos*B mutant mice shows exaggerated locomotor activation in response to initial cocaine exposures as well as robust CPP to a lower dose of cocaine compared with wild-type littermates (Hiroi et al., 1997). Changes in the balance of levels between proaddictive factors, such as bFGF, tPA, and BDNF, and anti-addictive factors, such as TNF-α, GDNF, CREB, and *Fos*B, induced by drugs of abuse seems to be important to the development of drug dependence. In the present study, the facilitation of METH-induced behavioral sensitization in mice with a targeted downregulation of shati highlights the opposing role of shati in drug-dependent behavioral plasticity. Therefore, upregulation of shati expression may represent a homeostastatic response of dopaminergic neurons in the NAc to excessive dopaminergic transmission, resulting in attenuation of hypersensitivity and CPP induced by METH-like drugs. Our findings, together with others, suggest that there are molecules in the brain that normally inhibit the behavioral actions of addictive substances. The mechanism underlying the upregulation of shati caused by METH remains to be elucidated; nevertheless, inhibitory feedback of the excessive DA signaling is likely to be a plausible candidate.

In conclusion, the present study established a functional interaction between shati and METH. Our findings suggest that shati is involved in the development of METH-induced hyperlocomotion, sensitization, and CPP, by promoting plasmalemmal and vesicular DA uptake as well as attenuating the METH-induced increase in overflow of DA in the NAc.

References

Ang E, Chen J, Zagouras P, Magna H, Holland J, Schaeffer E, Nestler EJ (2001) Induction of nuclear factor-κB in nucleus accumbens by chronic cocaine administration. J Neurochem 79:221–224.

Blackshaw S, Harpavat S, Trimarchi J., Cai L, Huang H, Kuo WP, Weber G, Lee K, Fraioli RE, Cho SH, Yung R, Asch E, Ohno-Machado L, Wong WH, Cepko CL (2004) Genomic analysis of mouse retinal development. PLoS Biol 2:E247.

Bowers MS, McFarland K, Lake RW, Peterson YK, Lapish CC, Gregory ML, Lanier SM, Kalivas PW (2004) Activator of G protein signaling 3: a gatekeeper of cocaine sensitization and drug seeking. Neuron 42:269–281.

Carlezon Jr WA, Thome J, Olson VG, Lane-Ladd SB, Brodkin ES, Hiroi N, Duman RS, Neve RL, Nestler EJ (1998) Regulation of cocaine reward by CREB. Science 282:2272–2275.

Cha XY, Pierce RC, Kalivas PW, Mackler SA (1997) NAC-1, a rat brain mRNA, is increased in the nucleus accumbens three weeks after chronic cocaine self-administration. J Neurosci 17:6864–6871.

Christensen AV, Arnt J, Hyttel J, Larsen JJ, Svendsen O (1984) Pharmacological effects of a specific dopamine D-1 antagonist SCH 23390 in comparison with neuroleptics. Life Sci 34:1529–1540.

Diatchenko L, Lau YF, Campbell AP, Chenchik A, Moqadam F, Huang B, Lukyanov S, Lukyanov K, Gurskaya N, Sverdlov ED, Siebert PD (1996) Suppression subtractive hybridization: a method for generating differentially regulated or tissue-specific cDNA probes and libraries. Proc Natl Acad Sci USA 93:6025–6030.

Di Chiara G, Imperato A (1988) Drugs abused by humans preferentially increase synaptic dopamine concentrations in the mesolimbic system of freely moving rats. Proc Natl Acad Sci USA 85:5274–5278.

Douglass J, Daoud S (1996) Characterization of the human cDNA and genomic DNA encoding CART: a cocaine- and amphetamine-regulated transcript. Gene 169:241–245.

Erickson JD, Masserano JM, Barnes EM, Ruth JA, Weiner N (1990) Chloride ion increases [^{3}H]dopamine accumulation by synaptic vesicles purified from rat striatum: inhibition by thiocyanate ion. Brain Res 516:155–160.

Fleckenstein AE, Metzger RR, Wilkins DG, Gibb JW, Hanson GR (1997) Rapid and reversible effects of methamphetamine on dopamine transporters. J Pharmacol Exp Ther 282:834–838.

Flores C, Samaha AN, Stewart J (2000) Requirement of endogenous basic fibroblast growth factor for sensitization to amphetamine. J Neurosci 20:RC55(1–5).

Franklin KBJ, Paxinos G (1997) The mouse brain: in stereotaxic coordinates. San Diego: Academic.

Giros B, Jaber M, Jones SR, Wightman PM, Caron MG (1996) Hyperlocomotion and indifference to cocaine and amphetamine in mice lacking the dopamine transporter. Nature 379:606–612.

Gurskaya NG, Diatchenko L, Chenchik A, Siebert PD, Khaspekov GL, Lukyanov KA, Vagner LL, Ermolaeva OD, Lukyanov SA, Sverdlov ED (1996) Equalizing cDNA subtraction based on selective suppression of polymerase chain reaction: cloning of Jurkat cell transcripts induced by phytohemaglutinin and phorbol 12-myristate 13-acetate. Anal Biochem 240:90–97.

Hall FS, Drgonova J, Goeb M, Uhl GR (2003) Reduced behavioral effects of cocaine in heterozygous brain-derived neurotropic factor (BDNF) knockout mice. Neuropsychopharmacology 28:1485–1490.

Heikkila RE, Orlansky H, Cohen G (1975) Studies on the distinction between uptake inhibition and release of ^{3}H-dopamine in rat brain tissue slices. Biochem Pharmacol 24:847–852.

Hiroi N, White NM (1991) The amphetamine conditioned place preference: differential involvement of dopamine receptor subtypes and two dopaminergic terminal areas. Brain Res 552:141–152.

Hiroi N, Brown JR, Haile CN, Ye H, Greenberg ME, Nestler EJ (1997) FosB mutant mice: loss of chronic cocaine induction of Fos-related proteins and heightened sensitivity to cocaine's psychomotor and rewarding effects. Proc Natl Acad Sci USA 94:10397–10402.

Horger BA, Iyasere CA, Berhow MT, Messer CJ, Nestler EJ, Taylor JR (1999) Enhancement of locomotor activity and conditioned reward to cocaine by brain-derived neurotropic factor. J Neurosci 19:4110–4122.

Koob GF (1992) Drugs of abuse: anatomy, pharmacology and function of reward pathways. Trends Pharmacol Sci 13:177–184.

Koob GF, Sanna PP, Bloom FE (1998) Neuroscience of addiction. Neuron 21:467–476.

Laakso A, Mohn AR, Gainetdinov RR, Caron MG (2002) Experimental genetic approaches to addiction. Neuron 36:213–228.

Larsen KE, Fon EA, Hastings TG, Edwards RH, Sulzer D (2002) Methamphetamine-induced degeneration of dopaminergic neurons involves autophagy and upregulation of dopamine synthesis. J Neurosci 22:8951–8960.

Liu Y, Edwards RH (1997) The role of vesicular transporter proteins in synaptic transmission and neural degeneration. Annu Rev Neurosci 20:125–156.

Lorrain DS, Arnold GM, Vezina P (2000) Previous exposure to amphetamine increases incentive to obtain the drug: long-lasting effects revealed by the progressive ratio schedule. Behav Brain Res 107:9–19.

McClung CA, Nestler EJ (2003) Regulation of gene expression and cocaine reward by CREB and ΔFosB. Nat Neurosci 6:1208–1215.

Melega WP, Williams AE, Schmitz DA, DiStefano EW, Cho AK (1995) Pharmacokinetic and pharmacodynamic analysis of the actions of D-amphetamine and D-methamphetamine on the dopamine terminal. J Pharmacol Exp Ther 274:90–96.

Messer CJ, Eisch AJ, Carlezon Jr WA, Whisler K, Shen L, Wolf DH, Westphal H, Collins F, Russell DS, Nestler EJ (2000) Role for GDNF in biochemical and behavioral adaptations to drugs of abuse. Neuron 26:247–257.

Mizoguchi H, Yamada K, Mizuno M, Mizuno T, Nitta A, Noda Y, Nabeshima T (2004) Regulations of methamphetamine reward by extracellular

signal-regulated kinase 1/2/ets-like gene-1 signaling pathway via the activation of dopamine receptors. Mol Pharmacol 65:1293–1301.
Mizoguchi H, Yamada K, Niwa M, Mouri A, Mizuno T, Noda Y, Nitta A, Itohara S, Banno Y, Nabeshima T (2007) Reduction of methamphetamine-induced sensitization and reward in matrix metalloproteinase-2 and -9-deficient mice. J Neurochem 100:1579–1588.
Nagai T, Yamada K, Yoshimura M, Ishikawa K, Miyamoto Y, Hashimoto K, Noda Y, Nitta A, Nabeshima T (2004) The tissue plasminogen activator-plasmin system participates in the rewarding effect of morphine by regulating dopamine release. Proc Natl Acad Sci USA 101:3650–3655.
Nagai T, Noda Y, Ishikawa K, Miyamoto Y, Yoshimura M, Ito M, Takayanagi M, Takuma K, Yamada K, Nabeshima T (2005a) The role of tissue plasminogen activator in methamphetamine-related reward and sensitization. J Neurochem 92:660–667.
Nagai T, Kamei H, Ito M, Hashimoto K, Takuma K, Nabeshima T, Yamada K (2005b) Modification by the tissue plasminogen activator-plasmin system of morphine-induced dopamine release and hyperlocomotion, but not anti-nociceptive effect in mice. J Neurochem 93:1272–1279.
Nagai T, Ito M, Nakamichi N, Mizoguchi H, Kamei H, Fukakusa A, Nabeshima T, Takuma K, Yamada K (2006) The rewards of nicotine: regulation by tissue plasminogen activator-plasmin system through protease activated receptor-1. J Neurosci 26:12374–12383.
Nakajima A, Yamada K, Nagai T, Uchiyama T, Miyamoto Y, Mamiya T, He J, Nitta A, Mizuno M, Tran MH, Seto A, Yoshimura M, Kitaichi K, Hasegawa T, Saito K, Yamada Y, Seishima M, Sekikawa K, Kim HC, Nabeshima T (2004) Role of tumor necrosis factor-α in methamphetamine-induced drug dependence and neurotoxicity. J Neurosci 24:2212–2225.
Napier TC, Givens BS, Schulz DW, Bunney BS, Breese GR, Mailman RB (1986) SCH23390 effects on apomorphine-induced responses of nigral dopaminergic neurons. J Pharmacol Exp Ther 236:838–845.
Nestler EJ (2001) Molecular basis of long-term plasticity underlying addiction. Nat Rev Neurosci 2:119–128.
Nestler EJ (2002) From neurobiology to treatment: progress against addiction. Nat Neurosci 5:1076–1079.
Niwa M, Nitta A, Shen L, Noda Y, Nabeshima T (2007a) Involvement of glial cell line-derived neurotrophic factor in inhibitory effects of a hydrophobic dipeptide Leu-Ile on morphine-induced sensitization and rewarding effects. Behav Brain Res 179:167–171.
Niwa M, Nitta A, Yamada Y, Nakajima A, Saito K, Seishima M, Shen L, Noda Y, Furukawa S, Nabeshima T (2007b) An inducer for glial cell line-derived neurotrophic factor and tumor necrosis factor-α protects against methamphetamine-induced rewarding effects and sensitization. Biol Psychiatry 61:890–901.
Niwa M, Nitta A, Yamada K, Nabeshima T (2007c) The roles of glial cell line-derived neurotrophic factor, tumor necrosis factor-α, and an inducer of these factors in drug dependence. J Pharmacol Sci, in press.
Niwa M, Nitta A, Yamada Y, Nakajima A, Saito K, Seishima M, Noda Y, Nabeshima T (2007d) Tumor necrosis factor-α and its inducer inhibit morphine-induced rewarding effects and sensitization. Biol Psychiatry, in press.
Noda Y, Miyamoto Y, Mamiya T, Kamei H, Furukawa H, Nabeshima T (1998) Involvement of dopaminergic system in phencyclidine-induced place preference in mice pretreated with phencyclidine repeatedly. J Pharmacol Exp Ther 286:44–51.
Robbins TW, Everitt BJ (1996) Neurobehavioural mechanisms of reward and motivation. Curr Opin Neurobiol 6:228–236.
Robinson TE, Berridge KC (1993) The neural basis of drug craving: an incentive-sensitization theory of addiction. Brain Res Brain Res Rev 18:247–291.
Satel SL, Southwick SM, Gawin FH (1991) Clinical features of cocaine-induced paranoia. Am J Psychiatry 148:495–498.
Schechter MD, Calcagnetti DJ (1998) Continued trends in the conditioned place preference literature from 1992 to 1996, inclusive, with a cross-indexed bibliography. Neurosci Biobehav Rev 22:827–846.
Seiden LS, Sabol KE, Ricaurte GA (1993) Amphetamine: effects on catecholamine systems and behavior. Annu Rev Pharmacol Toxicol 33:639–677.
Strakowski SM, Sax KW (1998) Progressive behavioral response to repeated d-amphetamine challenge: further evidence for sensitization in humans. Biol Psychiatry 44:1171–1177.
Strausberg RL, Feingold EA, Grouse LH, Derge JG, Klausner RD, Collins FS, Wagner L, Shenmen CM, Schuler GD, Altschul SF, Zeeberg B, Buetow KH, Schaefer CF, Bhat NK, Hopkins RF, Jordan H, Moore T, Max SI, Wang J, Hsieh F et al. (2002) Generation and initial analysis of more than 15,000 full-length human and mouse cDNA sequences. Proc Natl Acad Sci USA 99:16899–16903.
Sulzer D, Sonders MS, Poulsen NW, Galli A (2005) Mechanisms of neurotransmitter release by amphetamines: a review. Prog Neurobiol 75:406–433.
Taubenfeld SM, Milekic MH, Monti B, Alberini CM (2001) The consolidation of new but not reactivated memory requires hippocampal C/EBPβ. Nat Neurosci 4:813–818.
Uhl GR (1998) Hypothesis: the role of dopaminergic transporters in selective vulnerability of cells in Parkinson's disease. Ann Neurol 43:555–560.
Ujike H, Onoue T, Akiyama K, Hamamura T, Otsuki S (1989) Effects of selective D-1 and D-2 dopamine antagonists on development of methamphetamine-induced behavioral sensitization. Psychopharmacology 98:89–92.
Wada R, Tifft CJ, Proia RL (2000) Microglial activation precedes acute neurodegeneration in Sandhoff disease and is suppressed by bone marrow transplantation. Proc Natl Acad Sci USA 97:10954–10959.
Walters CL, Blendy JA (2001) Different requirements for cAMP response element binding protein in positive and negative reinforcing properties of drugs of abuse. J Neurosci 21:9438–9444.
Wang XB, Funada M, Imai Y, Revay RS, Ujike H, Vandenbergh DJ, Uhl GR (1997) rGβ1: a psychostimulant-regulated gene essential for establishing cocaine sensitization. J Neurosci 17:5993–6000.
Wise RA (1996a) Addictive drugs and brain stimulation reward. Annu Rev Neurosci 19:319–340.
Wise RA (1996b) Neurobiology of addiction. Curr Opin Neurobiol 6:243–251.
Wolf ME (1998) The role of excitatory amino acids in behavioral sensitization to psychomotor stimulants. Prog Neurobiol 54:679–720.
Yamada K, Nabeshima T (2004) Pro- and anti-addictive neurotrophic factors and cytokines in psychostimulant addiction: mini review. Ann NY Acad Sci 1025:198–204.
Yan Y, Yamada K, Niwa M, Nagai T, Nitta A, Nabeshima T (2007) Enduring vulnerability to reinstatement of methamphetamine-seeking behavior in glial cell line-derived neurotrophic factor mutant mice. FASEB J, in press.
Zachariou V, Bolanos CA, Selley DE, Theobald D, Cassidy MP, Kelz MB, Shaw-Lutchman T, Berton O, Sim-Selley LJ, Dileone RJ, Kumar A, Nestler EJ (2006) An essential role for ΔFosB in the nucleus accumbens in morphine action. Nat Neurosci 9:205–211.

ORIGINAL ARTICLE

Genome-Wide Association for Methamphetamine Dependence

Convergent Results From 2 Samples

George R. Uhl, MD, PhD; Tomas Drgon, PhD; Qing-Rong Liu, PhD; Catherine Johnson, MSc; Donna Walther, MSc; Tokutaro Komiyama, MD; Mutsuo Harano, MD; Yoshimoto Sekine, MD, PhD; Toshiya Inada, MD; Norio Ozaki, MD, PhD; Masaomi Iyo, MD, PhD; Nakao Iwata, MD, PhD; Mitsuhiko Yamada, MD; Ichiro Sora, MD, PhD; Chih-Ken Chen, MD, PhD; Hsing-Cheng Liu, MD, PhD; Hiroshi Ujike; Shih-Ku Lin, MD

Context: We can improve understanding of human methamphetamine dependence, and possibly our abilities to prevent and treat this devastating disorder, by identifying genes whose allelic variants predispose to methamphetamine dependence.

Objective: To find "methamphetamine dependence" genes identified by each of 2 genome-wide association (GWA) studies of independent samples of methamphetamine-dependent individuals and matched controls.

Design: Replicated GWA results in each of 2 case-control studies.

Setting: Japan and Taiwan.

Participants: Individuals with methamphetamine dependence and matched control subjects free from psychiatric, substance abuse, or substance dependence diagnoses (N=580).

Main Outcome Measures: "Methamphetamine dependence" genes that were reproducibly identified by clusters of nominally positive single-nucleotide polymorphisms (SNPs) in both samples in ways that were unlikely to represent chance observations, based on Monte Carlo simulations that corrected for multiple comparisons, and subsets of "methamphetamine dependence" genes that were also identified by GWA studies of dependence on other addictive substances, success in quitting smoking, and memory.

Results: Genes identified by clustered nominally positive SNPs from both samples were unlikely to represent chance observations (Monte Carlo $P<.00001$). Variants in these "methamphetamine dependence" genes are likely to alter cell adhesion, enzymatic functions, transcription, cell structure, and DNA, RNA, and/or protein handling or modification. Cell adhesion genes *CSMD1* and *CDH13* displayed the largest numbers of clustered nominally positive SNPs. "Methamphetamine dependence" genes overlapped, to extents much greater than chance, with genes identified in GWA studies of dependence on other addictive substances, success in quitting smoking, and memory (Monte Carlo P range $<.04$ to $<.00001$).

Conclusion: These data support polygenic contributions to methamphetamine dependence from genes that include those whose variants contribute to dependence on several addictive substances, success in quitting smoking, and mnemonic processes.

Arch Gen Psychiatry. 2008;65(3):345-355

METHAMPHETAMINE abuse is a growing problem in many regions of the United States and a long-standing concern in Taiwan and Japan. Elucidating which genetic variants enhance individuals' vulnerability should increase our understanding of methamphetamine dependence.

Recent reviews suggest that addictive substance dependence is likely to display a polygenic genetic architecture.[1-3] Psychostimulant dependence displays strong familial and genetic influences in family and twin studies.[4-18] Individual differences in vulnerability to methamphetamine are thus likely to display substantial genetic determinants. Since much of the genetic vulnerability to stimulant abuse overlaps with the genetics of vulnerability to other classes of addictive substances, it is likely that methamphetamine dependence displays such genetic overlaps as well.[13-16,19] However, there is no evidence that any single gene's variants mediate a large portion of vulnerability to psychostimulant dependence.

Identifying the genes that harbor allelic variants that contribute to human individual differences in vulnerabilities to methamphetamine dependence will help us to understand processes that underlie human addictions. We may improve understanding of the relative contributions of variants in the brain systems that underlie

Author Affiliations are listed at the end of this article.

Downloaded from www.archgenpsychiatry.com at Okayama University, on March 4, 2008
©2008 American Medical Association. All rights reserved.

reward vs mnemonic components of addictions, for example.[20] Increasing our ability to determine which constellation of genetic and environmental factors plays a role in the methamphetamine dependence of each affected individual should improve "personalized" targeting of treatment and prevention efforts to those most likely to benefit from them.

Genome-wide association (GWA) can help to elucidate chromosomal regions and genes that contain allelic variants that predispose to substance abuse. This approach does not require family member participation. It gains power as densities of genomic markers increase.[21-24] Association identifies smaller chromosomal regions than linkage-based approaches. Genome-wide association fosters pooling strategies that preserve confidentiality and reduce costs, including those that we have previously validated.[25-28] This approach provides ample genomic controls that can minimize the chances of unintended ethnic mismatches between disease and control samples (eg, stratification). The large numbers of assessments that are key components of GWA do mandate careful use of statistical approaches that correct for multiple comparisons and studies in multiple independent samples, such as those that we now report.

We thus now describe GWA in 2 samples of methamphetamine-dependent and control individuals. These studies test the a priori hypothesis that marker allele frequency differences between methamphetamine-dependent and control individuals will help us to identify genes whose alleles predispose to development of dependence on methamphetamine. Sample 1 contrasts (1) Han Chinese methamphetamine-dependent individuals from the Taipei region of Taiwan with (2) age- and sex-matched Han Chinese Taiwanese control individuals free from any histories of abuse or dependence on any legal or illegal addictive substance. Sample 2 contrasts (1) Japanese methamphetamine-dependent individuals with (2) age- and sex-matched Japanese control individuals free from any histories of abuse or dependence on any legal or illegal addictive substance. We used standard statistical approaches to document the power that these samples provided to identify genetic influences of different magnitudes. We identified striking convergence of the data from sample 1 and sample 2, in ways that are never attained by chance in many Monte Carlo simulation trials. We discuss the convergence that these data provide with recently reported GWA studies of related phenotypes that include polysubstance abuse, nicotine dependence, alcohol dependence, success in quitting smoking, and individual differences in memory. To our knowledge, these results provide the first replicated GWA study that identifies "methamphetamine dependence" genes.

METHODS

RESEARCH VOLUNTEERS

Sample 1

Subjects recruited in Taipei provided informed consent for genetic studies under protocols approved by ethics committees at the respective institutions; 30% were female and the mean (SD) age was 32.5 (10) years. One hundred forty individuals were diagnosed independently by each of 2 psychiatrists based on interviews, review of records, and Chinese versions of the Diagnostic Interview for Genetic Studies[29] and the Family Interview for Genetic Studies[30] using *DSM-IV* criteria.[31] These individuals were of ethnic Han Chinese origin and older than 17 years, reported methamphetamine use more than 20 times per year (unless they described well-documented methamphetamine psychosis), and denied histories of psychosis either prior to methamphetamine use or in relation to other psychedelic drugs. Most reported use of at least 1 other addictive substance. Two hundred forty Han Chinese controls, who were matched for sex and age, were older than 17 years, and denied either illegal drug use or psychotic symptoms to psychiatric interviewers, were recruited in Taipei from hospital and pharmacy staffs, blood donation centers, and an electric company.

Sample 2

Subjects who were born and resided in the northern Kyushu, Setouchi, Chiba, Tokai, or Kanto regions of Japan provided informed consent for genetic studies under protocols approved by ethics committees at the respective institutions. Twenty-one percent of subjects were female and the mean (SD) age was 39.9 (13) years. One hundred methamphetamine-dependent subjects were inpatients or outpatients of psychiatric hospitals in these regions that participate in the Japanese Genetics Initiative for Drug Abuse[32-45] and met *International Statistical Classification of Diseases, 10th Revision, Diagnostic Criteria for Research*[46] criteria F15.2 and F15.5 for methamphetamine dependence in independent diagnoses made by each of 2 trained psychiatrists based on interviews and review of records. Ninety-one percent revealed histories of methamphetamine psychosis, 89% used methamphetamine intravenously, 62% also abused organic solvents, and most abused at least 1 other substance. Subjects who displayed clinical diagnoses of schizophrenia, other psychotic disorders, or organic mental syndromes were excluded. Controls were 100 age-, sex-, and geographically matched staff recruited at the same institutions, who denied use of any illegal substance, abuse or dependence on any legal substance, any psychotic psychiatric illness, or any family history of substance dependence or psychotic psychiatric illness during interviews with trained psychiatrists.

DNA PREPARATION AND ASSESSMENT OF ALLELE FREQUENCIES

Genomic DNA was prepared from blood,[28,32,47,48] quantitated,[28,32] and combined into pools representing 20 individuals of the same ethnicity and phenotype. Relative allele frequencies were assessed using Affymetrix (Santa Clara, California) microarrays.

Hybridization probes were prepared from the genomic DNA pools (as described in the Affymetrix GeneChip Mapping Assay manual), with precautions to avoid contamination that included dedicated preparation rooms and hoods. Briefly, 50 ng of pooled genomic DNA was digested by *Xba*I or *Hind*III (100K) or by *Sty*I or *Nsp*I (500K), ligated to appropriate adaptors, and amplified using a GeneAmp PCR System 9700 (Applied Biosystems, Foster City, California) with a 3-minute 94°C hot start; 30 cycles of 30 seconds at 94°C, 45 seconds at 60°C, and 60 seconds at 68°C (100K) or 15 seconds at 68°C (500K); and a final 7-minute 68°C extension. Polymerase chain reaction (PCR) products were purified (MinElute 96 UF kits; Qiagen, Valencia, California) and quantitated. Forty micrograms of PCR product were digested for 35 minutes at 37°C with 0.04-unit/μL deoxyribonuclease I to produce 30– to 100–base pair fragments, which were end-labeled using terminal deoxynucleotidyl trans-

Downloaded from www.archgenpsychiatry.com at Okayama University, on March 4, 2008
©2008 American Medical Association. All rights reserved.

ferase and biotinylated dideoxynucleotides and hybridized to the appropriate 100K (*Xba*I or *Hind*III arrays) or 500K (*Sty*I or *Nsp*I arrays) array (early-access Centurion and commercial Mendel array sets; Affymetrix). Arrays were stained and washed as described in the Affymetrix GeneChip Mapping Assay manual using immunopure strepavidin (Pierce, Milwaukee, Wisconsin), biotinylated antistreptavidin antibody (Vector Labs, Burlingame, California), and R-phycoerythrin strepavidin (Molecular Probes, Eugene, Oregon). Arrays were scanned and fluorescence intensities were quantitated using an Affymetrix array scanner, as described previously.[28] Estimates for "genomic coverage" for these marker densities were almost 0.8 (sample 1) and almost 0.9 (sample 2).[49]

Chromosomal positions for each single-nucleotide polymorphism (SNP) were sought using NCBI (build 36.1; National Center for Biotechnology Information, Bethesda, Maryland) and NetAffyx (Affymetrix) data. Allele frequencies for each SNP in each DNA pool were assessed based on hybridization intensity signals from 4 arrays, allowing assessment of hybridization to the 20 (100K arrays) or 12 (500K arrays) "perfect match" cells on each array that were complementary to the PCR products from alleles "A" and "B" for each diallelic SNP on sense and antisense strands. We eliminated (1) SNPs with minor allele frequencies less than 0.02 determined using Affymetrix data; (2) SNPs on sex chromosomes; and (3) SNPs whose chromosomal positions could not be adequately determined. We thus analyzed data from the remaining 371 820 and 466 883 SNPs (for sample 1 and sample 2, respectively) in detail. Each array was analyzed, as described previously,[28] subtracting background values, normalizing to the highest values noted on the array, averaging the hybridization intensities from the array cells that corresponded to the perfect match "A" and "B" cells, calculating "A/B ratios" by dividing average normalized A values by average normalized B values, performing arctangent transformations to aid combination of data from arrays hybridized and scanned on different days, and determining the average arctan value for each SNP from the 4 replicate arrays. This approach is thus based on hybridization intensity data from Affymetrix scanners rather than relative allele score (RAS) or k corrections derived from RAS scores.[50,51]

The analyses presented in this work use standard methods for correcting hybridization values for each perfect match feature based on chip-to-chip differences in background fluorescence and in total fluorescence intensity. These approaches have generated good, approximately 0.95, correlations between individually genotyped and pooled-genotype values in extensive validation experiments.[32,52] Other approaches to analysis of pooling-based GWA studies have focused on the RAS measurements that derive from Affymetrix software to generate k correction scores for each SNP that attempt to correct for probe × probe variation (ie, that induced by, or consistent with, differential hybridization effects).[50,51] In studies that have used these corrections, correlations between individually and pooled genotyped SNP allelic frequencies can equal or exceed those that we have observed in validation experiments.[53,54] However, RAS scores have been used less and less as the genotype-calling algorithms for successive generations of Affymetrix arrays have improved their accuracy. Initial RAS scores are based in part on data from mismatch cells, which have again been eliminated from successive generations of Affymetrix arrays because of their inconsistent effects on accuracy. The k corrections based on RAS scores that are generated in different laboratories produce differing results.[55] Further, we have found that substantial numbers of the array features that provide information for the RAS scores are saturated under conditions used to conduct individual genotyping (Q-R.L., D.W., and G.R.U., unpublished data, 2005), leading us to use smaller amounts of input DNA and hybridization probes for the pooled assays reported herein. The k corrections may prove to be useful for experiments in which saturation is controlled carefully and where data from heterozygote control individuals are generated in the same experiments and in the same laboratories as the pooling data. However, in the present analysis, this adds to the variation that we already parse as quantified by replicate pools (ie, biological haplotype replication), applications of different chips to the same pool (ie, chip-oriented technical replication), and different samples altogether (ie, overall association replication).

ANALYSES

We compared data for all the pools from methamphetamine-dependent individuals with all of the pools from control individuals separately for sample 1 and sample 2, as previously described.[28] A *t* statistic for the differences between abusers and controls was generated, as described previously,[28] for each SNP for each sample. For each sample, we focused on "nominally positive" SNPs that displayed *t* statistics with $P < .05$ for abuser-control differences. We first sought evidence for clustering of the nominally positive SNPs from each sample. We focused on chromosomal regions in which at least 3 of these nominally positive SNPs, assessed by at least 2 different array types, lay within 25 kilobases (kb) of each other. We term these clustered nominally positive SNPs *clustered positive SNPs* and focus our analyses on regions in which they lie. The degree of clustering within each single sample provides a technical control (eg, assurance that there are haplotypes that occur at different frequencies in dependent vs control samples) that could result from stochastic differences in haplotypes as well as differences related to the methamphetamine-dependence phenotype.

To seek the SNPs within the strongest positive support from both data sets, we sought convergence between data from sample 1 and sample 2 (**Table**).[56] Analyses focused on genes identified by clustered positive results from both samples, rather than on individual SNPs whose informativeness might differ between samples 1 and 2. Clustering of positive results in the same gene in each of 2 independent samples is unlikely to represent purely stochastic effects for most genes and is thus likely to reflect differences related to dependence on methamphetamine (and/or to dependence on addictive substances in general).

Monte Carlo simulation trials assessed the significance of the results in ways that correct for the number of repeated comparisons made herein, as described previously.[28] These empirical statistical approaches do not require assumptions about the underlying distribution of the data sets, as do statistical approaches such as analysis of variance, and allow correction for the hundreds of thousands of repeated comparisons in ways that would provide difficulties for repeated analyses of variance. For each trial, a randomly selected set of SNPs from the current data set was assessed to see if it provided results equal to or greater than the results that we actually observed (eg, to see how frequently randomly selected sets of 15 565 SNPs from sample 1 and 25 538 SNPs from sample 2 contained nominally positive SNPs that lie clustered within 25 kb of each other on the chromosomes, see "Results" section). The number of trials for which the randomly selected SNPs displayed the same features of observed results was then tallied to generate an empirical *P* value. These simulations thus corrected for the number of repeated comparisons made in these analyses, an important consideration in evaluating this large association genome scanning data set. We used a similar approach to assess the likelihood that the convergences between the current data and data obtained from other samples might occur by chance.

To seek possible generalization of these results, we sought locations where the clustered positive data from both sample 1 and sample 2 lie at chromosomal positions near clustered positive results from studies that compared allelic frequencies in

Downloaded from www.archgenpsychiatry.com at Okayama University, on March 4, 2008
©2008 American Medical Association. All rights reserved.

Table. Selected "Methamphetamine Dependence" Genes Identified by Clustered Positive Results From Both Sample 1 and Sample 2[a]

Gene	Class	Description	SNPs[b]	*P* Value[c]
SGCZ	CAM	Sarcoglycan, zeta	3, 20	<.00001
DAF/CD55	ENZ	Decay-accelerating factor for complement system	1, 4	<.00001
ACSL6	ENZ	Acyl-CoA synthetase long-chain family member 6	9, 5	<.00001
FKBP15	ENZ	FKBP15	4, 4	<.00001
PDE6C	ENZ	cGMP phosphodiesterase 6C α′	4, 7	<.00001
POU5F1	TF	POU-domain 5 transcription factor 1	1, 5	<.00001
SH3MD4	PROT	SH3 multiple domains 4	9, 7	<.00001
RALY	RNA	Autoantigenic RNA binding protein	5, 3	<.00001
PRKG1	ENZ	cGMP-dependent protein kinase I	14, 5	.00001
LARGE	ENZ	Like-glycosyltransferase	11, 3	.00001
PCOLCE2	STR	Procollagen C endopeptidase enhancer 2	3, 2	.00001
MOSC2	ENZ	MOCO sulphurase C-terminal domain containing 2	4, 5	.00002
ZNF423	TF	Zinc finger protein 423	5, 4	.00002
MAP2K5	ENZ	Mitogen-activated protein kinase kinase 5	5, 3	.00003
USP48	PROT	Ubiquitin-specific peptidase 48	3, 2	.00003
SMYD3	TF	SET MYND domain containing 3	7, 5	.00007
CCHCR1	REC	Coiled-coil α-helical rod protein 1	2, 4	.00009
LRRN6C	CAM	Leucine-rich repeat neuronal 6C	4, 13	.00010
CENPC2	STR	Centromere protein C2	2, 3	.00012
RAPGEF5	REC	Rap guanine nucleotide exchange factor 5	4, 1	.00016
SERPINA5	ENZ	Serpin peptidase inhibitor A 5	4, 1	.00018
PRDM2	TF	PR domain containing 2 with ZNF domain	6, 3	.00022
ASTN2	CAM	Astrotactin 2	12, 3	.00037
TM7SF4	PROT	Transmembrane 7 superfamily member 4	2, 3	.00037
TRPM3	CHAN	Transient receptor potential cation channel, subfamily M, member 3	4, 10	.00039
RGS17	ENZ	Regulator of G-protein signaling 17	4, 3	.00047
COL28A1	STR	Collagen, type XXVIII, alpha 1	4, 3	.00047
MOSC1	ENZ	MOCO sulphurase C-terminal domain containing 1	5, 1	.00048
PDE4B	ENZ	Phosphodiesterase 4B	8, 4	.00049
AOAH	ENZ	Acyloxyacyl hydrolase	3, 4	.00049
PDE4D	ENZ	Phosphodiesterase 4D	6, 6	.00057
ZNF659	TF	Zinc finger protein 659	6, 9	.00060
NRG1	CAM	Neuregulin 1	5, 3	.00064
HS3ST4	ENZ	Heparan sulfate (glucosamine) 3-O-sulfotransferase 4	3, 7	.00064
MYO5B	STR	Myosin 5B	4, 11	.00065
PSD3	REC	Pleckstrin and sec7 domain containing 3	3, 15	.00078
AK5	ENZ	Adenylate kinase 5	6, 3	.00080
CUBN	REC	Cubilin	6, 6	.00085
FHIT	ENZ	Fragile histidine triad gene	8, 20	.00088

Abbreviations: Acyl-CoA, acyl coenzyme A; CAM, cell adhesion molecule; cGMP, cyclic guanine monophosphate; CHA, channels; DIS, disease associated; ENZ, enzymes; PROT, protein processing; REC, receptors (combining single TM, 7 TM, and ligand-gated channel families); RNA/DNA, RNA/DNA handling or modification; SNP, single-nucleotide polymorphism; STR, structural proteins; TF, transcriptional regulation; TRANSP, transporter.

[a]Each gene listed here contains at least 5 clustered positive SNPs with $P < .05$ from sample 1 and/or sample 2, has a function that can be inferred, and displays a Monte Carlo *P* value <.001. Genes are grouped by the class of the function to which they appear to contribute: CAM, ENZ, STR, TF, PROT, REC, RNA/DNA, TRANSP, CHA, and DIS. The Monte Carlo *P* value represents probabilities of chance discovery of clustered nominally positive SNPs in segments of randomly selected genes that sum to the same size as the true gene identified in the present work. Genes listed in this Table are selected because their Monte Carlo *P* values are <.001 and/or because they are identified in other samples in ways that are discussed in the text (see eTable [available at http://www.archgenpsychiatry.com] for full table, in which correction for 109 repeated comparisons would require $P < .0004$ for significance).

[b]Numbers of clustered nominally positive SNPs from samples 1 and 2 that lie within the gene's exons or 10-kilobase flanks.

[c]Monte Carlo *P* value for the number of nominally significant SNPs lying within a gene region of the same size.

polysubstance abusers vs controls,[32] alcohol-dependent individuals vs controls,[57] nicotine-dependent individuals vs nondependent smokers,[58] individuals successful in quitting smoking vs those unsuccessful,[59] and individuals with better or poorer scores in memory testing[55] (Table).

To provide controls for the alternative possibilities that the results obtained herein could come from (1) occult racial/ethnic stratification or (2) assay noise, we compared the clustered positive SNPs from sample 1 and from sample 2 with SNPs that displayed the largest allele frequency differences between (1) European American vs African American control individuals, as previously described[32]; (2) HapMap Japanese (JPT) and Han Chinese (HCB) samples; and (3) SNPs that displayed the largest variances from array to array, as previously described.[32]

To assess the statistical power of our analysis, we used the program PS version 2.1.31[60] with (1) $\alpha = .05$, (2) sample sizes equal to the numbers of pools from the current data set, (3) mean abuser-control differences of 0.05 and 0.1, and (4) standard deviations from the SNPs that provided the largest differences between control and abuser population means from the current data set. We also present data from the Genetic Power Calculator.

Power Calculations

There is no single standard for calculation of the power of GWA; we have thus presented calculations based on allele frequency differences in the body of this article. An alternative approach,

Downloaded from www.archgenpsychiatry.com at Okayama University, on March 4, 2008
©2008 American Medical Association. All rights reserved.